

1 Intrinsic excitability in layer IV-VI anterior insula to basolateral
2 amygdala projection neurons encodes the confidence of taste
3 valence

4

5 Sailendrakumar Kolatt Chandran^{1, *}, Adonis Yiannakas^{1, 3, *}, Haneen Kayyal¹,
6 Randa Salalha¹, Federica Cruciani¹, Liron Mizrahi¹, Mohammad Khamaisy¹, Shani
7 Stern¹, Kobi Rosenblum^{1,2}

8

9 ¹Sagol Department of Neurobiology, University of Haifa, Mount Carmel, Haifa, Israel

10 ²Center for Gene Manipulation in the Brain, University of Haifa, Mount Carmel, Haifa, Israel

11 ³Institute of Biochemistry and Molecular Medicine, University of Bern, Bern, Switzerland

12 *Authors contributed equally to this work

13

14 Correspondence

15 Prof. Kobi Rosenblum, Ph.D.

16 Sagol Department of Neurobiology

17 University of Haifa

18 Haifa, 3498838, Israel

19 kobir@psy.haifa.ac.il

20

21 Dr. Adonis Yiannakas, Ph.D.

22 Institute of Biochemistry and Molecular Medicine

23 University of Bern,

24 Bern, 3012, Switzerland

25 adonis.yiannakas@gmail.com

26

27 Dr. Sailendrakumar Kolatt Chandran, Ph.D.

28 Sagol Department of Neurobiology

29 University of Haifa

30 Haifa, 3498838, Israel

31 sailendrakumarkc@gmail.com

32 Word Count

33 Abstract: 197

34 Introduction: 800

35 Materials and methods: 2475

36 Results: 3968

37 Discussion: 1766

38

39 Abstract

40 Avoiding potentially harmful, and consuming safe food is crucial for the survival of living
41 organisms. However, sensory information can change its valence following conflicting
42 experiences. Novelty and aversiveness are the two crucial parameters defining the currently
43 perceived valence of taste. Importantly, the ability of a given taste to serve as CS in conditioned
44 taste aversion (CTA) is dependent on its valence. Activity in anterior insula (aIC) layer IV-VI
45 pyramidal neurons projecting to the basolateral amygdala (BLA) is correlative and necessary for
46 CTA learning and retrieval, as well as the expression of neophobia towards novel tastants, but not
47 learning taste familiarity. Yet, the cellular mechanisms underlying the updating of taste valence
48 representation in this specific pathway are poorly understood. Here, using retrograde viral tracing
49 and whole cell patch-clamp electrophysiology in trained mice, we demonstrate that the intrinsic
50 properties of deep-lying layer IV-VI, but not superficial layer I-III aIC-BLA neurons, are
51 differentially modulated by both novelty and valence, reflecting the subjective predictability of
52 taste valence arising from prior experience. These correlative changes in the profile of intrinsic
53 properties of LIV-VI aIC-BLA neurons were detectable following both simple taste experiences,
54 as well as following memory retrieval, extinction learning and reinstatement.

55

56 Introduction

57 In the natural setting, animals approach novel taste stimuli tentatively, as to closely examine
58 them according to a genetic plan, as well as in relation to associated visceral consequences
59 (Schier and Spector, 2019). Bitter and sour tastes are innately aversive, acting as warning signals
60 for the presence of toxins (Bachmanov et al., 1996). Conversely, neophobia to innately appetitive
61 sweet and moderately salty tastants dissipates over time (Lin et al., 2012). Importantly, animals
62 can learn to avoid innately appetitive tastants (e.g., saccharin-, or NaCl-water – the conditioned
63 stimulus, CS), through conditioned taste aversion - CTA (Garcia et al., 1955; Nachman and Ashe,
64 1973). This single-trial associative learning paradigm results in robust aversion following the
65 pairing of the CS with a malaise-inducing agent (the unconditioned stimulus, US), such as LiCl
66 (Bures et al., 1998). CTA memories are robust, but can be extinguished through unreinforced CS
67 re-exposures, and subsequently reinstated through US re-exposure (Schachtman et al., 1985;
68 Mickley et al., 2004). Unlike other forms of classical conditioning, the inter-stimulus interval
69 (ISI) between taste experience (CS) and visceral outcome (US), extends to several hours
70 (Adaikkan and Rosenblum, 2015). How CTA learning enables this long-trace associative
71 process, within timeframes that deviate from classical Hebbian plasticity mechanisms is
72 currently unknown (Chinnakkaruppan et al., 2014; Adaikkan and Rosenblum, 2015).

73 The primary taste cortex - the anterior insula (aIC), along with the basolateral amygdala (BLA),
74 govern the encoding and retrieval of taste information (Piette et al., 2012; Bales et al., 2015).
75 Gustatory processing at the IC encompasses thalamocortical and corticocortical inputs that relay
76 taste-, as well as palatability-related inputs from the BLA, that reflect the emotional valence
77 associated with taste stimuli (Stone et al., 2020). Neuronal taste responses at the IC and BLA are
78 using temporal information to encode multiple types of information relating to stimulus identity

79 and palatability (Grossman et al., 2008; Sadacca et al., 2012; Arieli et al., 2020; Vincis et al.,
80 2020). Both synaptic plasticity and neuronal intrinsic properties are proposed to serve as cellular
81 mechanisms underlying learning and memory (Citri and Malenka, 2008; Sehgal et al., 2013).
82 CTA learning promotes LTP induction in the BLA-IC pathway (Jones et al., 1999; Juárez-
83 Muñoz et al., 2017), and strengthens cell-type specific functional connectivity along the
84 projection (Haley et al., 2016). Intrinsic excitability is the tendency of neurons to fire action
85 potentials when exposed to inputs, reflecting changes in the suit and properties of specific ion
86 channels (Disterhoft et al., 2004; Song and Moyer, 2018). Even though independent mechanisms
87 are involved, recent evidence indicates learning and memory necessitates the that coupling of
88 intrinsic and synaptic plasticity (Turrigiano, 2011; Greenhill et al., 2015; Wu et al., 2021).

89 The IC is an integration hub tuned for the encoding of both exteroceptive as interoceptive
90 information (Gogolla et al., 2014; Haley and Maffei, 2018; Livneh et al., 2020; Koren et al.,
91 2021). By virtue of its extensive network of connectivity, this elongated cortical structure has
92 been shown to integrate sensory, emotional, motivational, and cognitive brain centers through
93 distinct mechanisms. For example, deletions of either *Fos* or *Stk11* in BLA-aIC neurons, alter
94 intrinsic properties at the aIC, and impair CTA acquisition (Levitan et al., 2020). Furthermore,
95 approach behaviors in social decision-making are modulated by subjective and sex-specific
96 affective states that regulate cell-type-specific changes in intrinsic properties at IC terminals
97 receiving hypothalamic input (Rogers-Carter et al., 2018, 2019; Rieger et al., 2022). The
98 posterior IC (pIC) integrates visceral-sensory signals of current physiological states with
99 hypothalamus-gated amygdala anticipatory inputs relating to food or water ingestion, to predict
100 future physiological states (Livneh et al., 2017, 2020). Conversely, aversive visceral stimuli such
101 as LiCl, activate CaMKII neurons projecting to the lateral hypothalamus in right-, but not the left

102 IC, whose optogenetic activation or inhibition can bidirectionally regulate food consumption
103 (Wu et al., 2020). We have previously shown that the aIC-BLA projection is necessary and
104 sufficient for CTA acquisition and retrieval (Lavi et al., 2018; Kayyal et al., 2019), while CTA
105 retrieval requires activation of the projection concomitant with parvalbumin (PV) interneurons
106 (Yiannakas et al., 2021). Moreover, artificial activation of aIC-BLA projecting neurons is
107 sufficient to induce CTA for appetitive taste (Kayyal et al., 2019). Here, using retrograde viral
108 tracing, behavioral analysis, and whole-cell patch-clamp slice electrophysiology, we assessed
109 two hypotheses: (1) That the intrinsic properties of the aIC-BLA projection change as a function
110 of certainty of taste valence prediction, but not percept; and (2) that predictive valence-specific
111 changes in intrinsic properties would be reflected through excitability, being low when taste
112 outcome is highly predictive (i.e., following CTA retrieval or unreinforced familiarization), and
113 high when taste valence is uncertain (i.e., following novelty or extinction). Our data demonstrate
114 for the first time that the intrinsic properties of LIV-VI aIC-BLA neurons are differentially
115 regulated by innate and learned drives, reflecting the confidence of currently perceived taste
116 valence.

117

118 **Materials and methods**

119 **Animals**

120 Animals used were 8–12-week-old C57BL/6j (WT) adult male mice. Mice were kept in the local
121 animal resource unit at the University of Haifa on a 12-hour dark/light cycle. Water and chow
122 pellets were available ad libitum, while ambient temperature was tightly regulated. All
123 procedures conducted were approved by the University of Haifa Animal Care and Use

124 Committee (Ethics License 554/18), as prescribed by the Israeli National Law for the Protection
125 of Animals – Experiments with Animals (1994).

126

127 Animal surgery and viral injections

128 Following surgery and stereotactic injection of viral vectors, behavioral paradigms were
129 performed, as previously described (Yiannakas et al., 2021). Briefly, mice were treated with
130 norocarp (0.5mg/kg), before being anesthetized (M3000 NBT Israel/Scivena Scientific) and
131 transferred to a Model 963 Kopf® stereotactic device. Upon confirming the lack of pain
132 responses, the skull was surgically exposed and drilled to bilaterally inject 0.25µl of
133 ssAAV_retro2-hSyn1-chi-mCherry-WPRE-SV40p(A) (physical titer 8.7 x 10E12 vg/ml), at the
134 BLA (AP -1.58; ML ± 3.375; DV - 4.80). Viral delivery was performed using a Hamilton micro-
135 syringe (0.1µL/minute), while the sculp was cleaned and closed using Vetbond®. Animals were
136 then administered with 0.5mg/kg norocarp and 0.5mg/kg of Baytril (enrofloxacin), and then
137 transferred to a clean and heat-adjusted enclosure for 2 hours. Upon inspection, mice were
138 returned to fresh cages along with similarly treated cage-mates. Weight-adjusted doses of the
139 Norocarp and Baytril were administered for an additional 3 days. All AAV constructs used in this
140 study were obtained from the Viral Vector Facility of the University of Zurich
141 (<http://www.vvf.uzh.ch/>).

142

143 Electrophysiological studies of the influence of innate taste identity, novelty, and valence
144 on aIC-BLA excitability

145 WT mice treated with viral constructs labeling aIC-BLA projecting neurons were used for

146 electrophysiological studies. Upon recovery, mice were randomly assigned into treatment groups
147 (Figure 1). Following 24hrs of water deprivation, animals were water restricted for 3 days,
148 receiving water in pipettes ad libitum for 20 minutes/day (Kayyal et al., 2019; Yiannakas et al.,
149 2021). This regime has been extensively used by our lab as it allows rodents to reliably learn to
150 drink from water pipettes with minimal weight loss. Mean total drinking was recorded on the 3rd
151 day of water restriction. Novel taste consumption groups were presented with 1.0mL of either
152 0.5% saccharin (*Saccharin 1x*), or Quinine 0.014% (*Quinine 1x*). One hour following the final
153 taste presentation, animals were subjected to patch-clamp electrophysiology (Kayyal et al., 2021;
154 Yiannakas et al., 2021). The *Water* group underwent the same behavioral procedure without
155 novel taste presentations were sacrificed for electrophysiological investigations one hour
156 following water presentation. To dissociate between taste identity and familiarity-related changes
157 in electrophysiological properties, a cohort of mice treated to label the aIC-BLA projection were
158 similarly water deprived following familiarization with saccharin (*Saccharin 5x*). Following the
159 initial water restriction, *Saccharin 5x* animals were allowed access to 0.5% saccharin, in
160 20minute sessions for 4 days. On the fifth day, mice were provided with 1.0ml of the tastant, 1
161 hour prior to sacrifice for electrophysiological recordings. Additionally, WT animals injected
162 with the same viral vector, were allowed a month to recover, following which they were
163 sacrificed for electrophysiological investigations without any behavioral manipulation (*Cage*
164 *Controls*).

165

166 Electrophysiological studies of the influence of learned aversive taste memory retrieval
167 on aIC-BLA excitability

168 WT mice were treated with viral constructs labelling aIC-BLA projecting neurons to assess the

169 electrophysiological properties of the projection during aversive or appetitive taste memory
170 retrieval. Upon recovery, mice in CTA retrieval group were trained in CTA for saccharin (LiCl
171 0.14M, 1.5% body weight), while the appetitive saccharin retrieval group (*Saccharin 2x*)
172 received a matching body weight adjusted injection of saline (Yiannakas et al., 2021). Three days
173 following conditioning, both groups underwent a memory retrieval task, receiving 1.0mL of the
174 conditioned tastant 1 hour prior to sacrifice (Figures 2, 4). Brain tissue was extracted and
175 prepared for electrophysiological recording, as above.

176

177 Electrophysiological studies of the influence of learned aversive taste memory extinction
178 and reinstatement on aIC-BLA excitability

179 Electrophysiological studies of CTA extinction and reinstatement were conducted in a cohort of
180 WT male mice (Yiannakas et al., 2021). Following surgery, recovery and water restriction,
181 animals were randomly assigned to the extinction and reinstatement groups (Figures 3-4). Adult
182 male mice used to study extinction and reinstatement were trained in CTA for saccharin
183 following extinction, the reinstatement group received an identical intraperitoneal dose to the
184 original unconditioned stimulus (LiCl 0.14M, 1.5% body weight), 24 hours prior to retrieval.
185 Conversely, the extinction group received a similarly weight-adjusted dose of saline. During the
186 final retrieval session, both groups of mice were allowed access to 1.0mL of the CS, 1 hour prior
187 to sacrifice under deep anesthesia and slice preparation for electrophysiology.

188

189 Electrophysiology tissue preparation

190 The slice electrophysiology and recording parameters were used as described previously (Kayyal

191 et al., 2021; Yiannakas et al., 2021). Briefly, mice were deeply anesthetized using isoflurane,
192 while brains were extracted following decapitation. Three-hundred um thick coronal brain slices
193 were obtained with a Campden-1000® Vibratome. Slices were cut in ice-cold sucrose-based
194 cutting solution containing the following (in mM): 110 sucrose, 60 NaCl, 3 KCl, 1.25 NaH₂PO₄,
195 28 NaHCO₃, 0.5 CaCl₂, 7 MgCl₂, 5 D-glucose, and 0.6 ascorbate. The slices were allowed to
196 recover for 30 min at 37°C in artificial CSF (ACSF) containing the following (in mM): 125
197 NaCl, 2.5 KCl, 1.25 NaH₂PO₄, 25 NaHCO₃, 25 D-glucose, 2 CaCl₂, and 1 MgCl₂. Slices were
198 then kept for an additional 30 min in ACSF at room temperature until electrophysiological
199 recording. The solutions were constantly gassed with carbogen (95% O₂, 5% CO₂).

200

201 Intracellular whole cell recording

202 After the recovery period, slices were placed in the recording chamber and maintained at 32-
203 34°C with continuous perfusion of carbogenated ACSF (2 ml/min). Brain slices containing the
204 anterior insular cortices were illuminated with infrared light and pyramidal cells were visualized
205 under a differential interference contrast microscope with 10X or 40X water-immersion
206 objectives mounted on a fixed-stage microscope (BX51-WI; Olympus®). The image was
207 displayed on a video monitor using a charge-coupled device (CCD) camera (QImaging®,
208 Canada). Insula to BLA projection cells infected with AAV were identified by visualizing
209 mCherry⁺ cells. Recordings were amplified by Multiclamp™ Axopatch™ 200B amplifiers and
210 digitized with Digidata® 1440 (Molecular Devices®). The recording electrode was pulled from a
211 borosilicate glass pipette (3–5 M) using an electrode puller (P-1000; Sutter Instruments®) and
212 filled with a K-gluconate-based internal solution containing the following (in mM): 130 K-
213 gluconate, 5 KCl, 10 HEPES, 2.5 MgCl₂, 0.6 EGTA, 4 Mg-ATP, 0.4 Na₃GTP and 10

214 phosphocreatine (Na salt). The osmolarity was 290 mOsm, and pH was 7.3. The recording glass
215 pipettes were patched onto the soma region of mCherry⁺ pyramidal neurons and neighboring non
216 fluorescent pyramidal neurons.

217 The recordings were made from the soma of insula pyramidal cells, particularly from layer 2/3
218 and Layer 5/6. Liquid junction potential (10 mV) was not corrected online. All current clamp
219 recordings were low pass filtered at 10 kHz and sampled at 50 kHz. Pipette capacitance and
220 series resistance were compensated and only cells with series resistance smaller than 20 MΩ
221 were included in the dataset. The method for measuring active intrinsic properties was based on a
222 modified version of previous protocols (Kaphzan et al., 2013; Chakraborty et al., 2017; Sharma
223 et al., 2018).

224

225 Recording parameters

226 Resting membrane potential (RMP) was measured 10 sec after the beginning of whole cell
227 recording (rupture of the membrane under the recording pipette). The dependence of firing rate
228 on the injected current was obtained by injection of current steps (of 500ms duration from 0 to
229 400 pA in 50 pA increments). Input resistance was calculated from the voltage response to a
230 hyperpolarizing current pulse (-150 pA). SAG ratio was calculated from voltage response -150
231 pA. The SAG ratio during the hyperpolarizing steps was calculated as $[(1 - \Delta V_{SS} / \Delta V_{max}) \times$
232 $100\%]$ as previously reported by (Song, Ehlers, & Moyer, 2015). The membrane time constant
233 was determined using a single exponential fit in the first 100ms of the raising phase of cell
234 response to a 1 second, -150 pA hyperpolarization step.

235 For measurements of a single action potential (AP), after initial assessment of the current

236 required to induce an AP at 15ms from the start of the current injection with large steps (50 pA),
237 a series of brief depolarizing currents were injected for 10ms in steps of 10 pA increments. The
238 first AP that appeared on the 5ms time point was analyzed. A curve of dV/dt was created for that
239 trace and the 30 V/s point in the rising slope of the AP was considered as threshold (Chakraborty
240 et al., 2017). AP amplitude was measured from the equipotential point of the threshold to the
241 spike peak, whereas AP duration was measured at the point of half-amplitude of the spike. The
242 medium after-hyperpolarization (mAHP) was measured using prolonged (3 seconds), high-
243 amplitude (3 nA) somatic current injections to initiate time-locked AP trains of 50 Hz frequency
244 and duration (10 –50 Hz, 1 or 3 s) in pyramidal cells. These AP trains generated prolonged (20 s)
245 AHPs, the amplitudes and integrals of which increased with the number of APs in the spike train.
246 AHP was measured from the equipotential point of the threshold to the anti-peak of the same
247 spike (Gulledge et al., 2013). Fast (fAHP), and slow AHP (sAHP) measurements were identified
248 as previously described (Andrade et al., 2012; Song and Moyer, 2018). Series resistance, R_{in} ,
249 and membrane capacitance were monitored during the entire experiment. Changes of at least
250 30% in these parameters were criteria for exclusion of data.

251 Classification of Burst and Regular spiking neurons

252 At the end of recordings, neurons were classified as either burst (BS) or regular spiking (RS) as
253 reported previously (Kim et al., 2015; Song et al., 2015). Briefly, neurons that fired two or more
254 action potentials (doublets or triplets) potential towards a depolarizing current step above the
255 spike threshold current were defined as burst spiking (BS). Regular spiking (RS) neurons on the
256 other hand, were defined as neurons that fired single action potential in response to a
257 depolarizing current step above spike threshold (Extended Figure 1-2A).

258

259 Statistical analysis of individual intrinsic properties across treatments

260 Individual intrinsic properties of aIC-BLA projecting neurons in the respective treatment groups
261 (Figures 1-4) were analyzed using appropriate statistical tests (One-way or Two-way ANOVA,
262 GraphPad Prism®), as defined in the Statistics Table. Two-way repeated measurements of
263 analysis of variance (RM-ANOVA) followed by Sidak's (for two groups) or Tukey's (for more
264 than two groups) post-hoc multiple comparison test was performed for firing properties. The
265 intrinsic properties were determined with Two-tailed unpaired t-tests, and One-way ANOVA
266 followed by Tukey's or Dunn's multiple comparisons test were used. For all tests, * $p < 0.05$ was
267 considered significant. Following spike-sorting, the ratio of BS:RS aIC-BLA projecting neurons
268 in the sampled population was compared across our treatments (Mann-Whitney test, GraphPad
269 Prism®). Similarly, individual intrinsic properties in BS and RS aIC-BLA projecting neurons
270 were analyzed following spike-sorting (One-way or Two-way ANOVA, GraphPad Prism®). All
271 data reported as mean \pm standard error (SEM).

272

273 Immunohistochemistry

274 From each electrophysiological recording, three 300 μ m-thick mouse brain slices were obtained
275 starting from Bregma coordinates 1.78, 1.54 and 1.18, respectively. Slices were washed with
276 PBS and fixed using 4% paraformaldehyde in PBS at 4⁰C for 24 hours. Slices were then
277 transferred to 30% sucrose/PBS solution for 48 hours and mounted on glass slides using
278 Vectashield® mounting medium with DAPI (H-1200). Slides were then visualized using a
279 vertical light microscope at 10x and 20x magnification (Olympus CellSens Dimension®).
280 Images were processed using Image-Pro Plus® V-7 (Media Cybernetics). The localization of
281 labelled mCherry⁺ neurons in the agranular aIC - where recordings were obtained from, was

282 quantified manually across three Bregma-matched slices, for each animal. Quantification was
283 done using randomly assigned IDs for individual animals, regardless of treatment.
284 Representative images were additionally processed using the Olympus CellSens 2-D
285 deconvolution® function.

286

287 Principal component analysis (PCA) of the profile of intrinsic properties across treatment
288 groups

289 Principal component analysis (PCA) of the standardized intrinsic properties of the LIV-VI aIC-
290 BLA (Figure 5; Extended Figure 5-1) was performed using the correlation matrix on GraphPad
291 Prism9, MATLAB R2020b, and IBM SPSS Statistics 27. The covariance matrix was used for
292 each PCA was performed in six behavioral groups, the low memory prediction (Saccharin 1x,
293 n=20; Saccharin 2x, n=20, and Extinction, n=14), and the high memory prediction (Saccharin 5x,
294 n=18; CTA retrieval, n=27, and Reinstatement, n=15), RS vs. BS neurons. A total of 114 neurons
295 (BS vs. RS) across all intrinsic properties and excitability changes (50–400 pA) (Extended
296 Figure 5-1A), and later all intrinsic properties with only 350 pA (highest excitability differences
297 between treatment groups; Extended Figure 5-1, B). PCA was conducted on 63 burst spiking
298 neurons using 12 variables: 350 (pA), RMP (mV), mAHP (mV), sAHP (mV), fAHP (mV), IR
299 (MΩ), Sag Ratio, Time constants (msec), AP amplitude (mV), AP Halfwidth (msec), AP
300 threshold (mV), Rheobase (pA), (Figure 5 A &B). The adequacy of the sample was evaluated
301 using the Bartlett's test and the Kaiser-Meyer-Olkin (KMO) measure was applied. The degrees
302 of freedom (df) were calculated using the following formula:

$$df = \#variables - 1.$$

303 The number of principal components was chosen according to the percentage of variance

304 explained (>75%). The parallel analysis evaluated the optimal number of components and
305 selected 3 PCs, explaining 62.47% of the variance. Oblique factor rotation (par) of the first three
306 PCA components, using a standard 'rotatefactors' routine from MATLAB Statistics Toolbox.
307 This approach maximizes the varimax criterion using an orthogonal rotation. To optimize
308 variance, oblique factor rotation (paramax) was used, and the threshold chosen to define a
309 variable as a significant contributor was a variance ≥ 0.7 given the small sample size. The
310 correlation matrix was adequate as the null hypothesis of all zero correlation was rejected
311 [$\chi^2_{66}=387.444$, $p<0.001$], and KMO exceeded 0.5 (KMO=0.580).

312 To calculate the proportion of the variance of each variable that the principal components can
313 explain, communalities were calculated and ranged from 0.426 to 0.897 (extended Figure 5-1, -A
314 C). The communalities scores were calculated using the following formula: $= \frac{\sum_{i=1}^m \lambda}{\#variables * \lambda}$; where
315 m is the number of selected PCs. The threshold chosen was $Comm \geq 60\%$.

316 Due to the imbalance in sample sizes between groups, the PCA space is biased in favor of the
317 group with bigger sample size. The BS neurons in the six behavioral groups previously men-
318 tioned were resampled to ensure that sample sizes were balanced across groups datasets (Figure
319 5, A&B). Particularly, we reduced the number of Saccharin 1X and 2X observations by using
320 random sampling ("randn" function in MATLAB); for Saccharin 1x, we chose 10 of the 17 total
321 elements, and for Saccharin 2x, we selected 10 of the 13 total elements.

322 **K-means clustering**

323 To assess the distribution of bursting neurons in multidimensional space, we performed a k-
324 means cluster analysis in MATLAB (k = 2 clusters, maximum iterations was 100 with random
325 starting locations, squared Euclidean distance metric used) for the principal components, which
326 explained 62.47% of the variance in intrinsic properties (Figure 5; extended Figure 5-1 and 5-2).

327

328 Results

329 To prove or refute our hypotheses, we conducted a series of electrophysiological recordings in
330 slice preparation from the mouse aIC, in which we labelled aIC-BLA projecting neurons using
331 retrograde adeno-associated viral tracing – retro AAV (see Methods). Electrophysiological
332 recordings were obtained from the aIC-BLA projecting neurons in LI-III (Table 2) and LIV-VI
333 (Table 1), following novel appetitive or aversive taste stimuli (Figure 1), following appetitive or
334 aversive taste memory retrieval (Figure 2), as well as following extinction and reinstatement
335 (Figures 3-4). We focused on deep-lying LIV-VI aIC-BLA projecting neurons (Table 1), as
336 intrinsic properties in superficial LI-III aIC-BLA projecting neurons were unaffected by taste
337 identity, familiarity, or valence (Table 2). We measured action potential (AP) firing frequency in
338 response to incrementally increasing depolarizing current injections, as well as 11 distinct of
339 intrinsic properties (Tables 1-2 and Statistics Table): resting membrane potential (RMP); slow,
340 medium and fast after-hyperpolarization (sAHP, mAHP, fAHP); input resistance (IR), SAG
341 ratio; the amplitude, half-width and threshold for APs; the time taken for a change in potential to
342 reach 63% of its final value (membrane time constant - τ), as well as the minimum current
343 necessary for AP generation (Rheobase). Statistical analysis was conducted using repeated
344 measures one- or two-way ANOVA (see Statistics table).

345

346 When taste is both appetitive and novel, excitability in LIV-VI aIC-BLA projection
347 neurons is increased

348 To delineate the mechanisms through which novelty is encoded on the LIV/VI aIC-BLA

349 projection, we labeled the projection (see methods), and compared the intrinsic properties across
350 neutral, innately aversive, and innately appetitive taste stimuli. Following surgery recovery mice
351 were randomly assigned to the following behavioral groups: Water (Control for procedure,
352 Water; n=6 animals, 23 cells), 0.5 % Saccharin for the first (Novel innate appetitive, Saccharin
353 1x; n=5 animals, 20 cells), or fifth time (Familiar appetitive, Saccharin 5x; n=6 animals, 18
354 cells), 0.04% Quinine (Novel aversive, Quinine 1x; n=4 animals, 19 cells), or cage controls that
355 did not undergo water-restriction (Base-line control, Cage control; n=4 animals, 19 cells). This
356 approach allowed us to examine excitability changes that relate to the innate aversive/appetitive
357 nature and novelty/familiarity associated with tastants, while accounting for the effects of acute
358 drinking, as well as the water restriction regime itself. Guided by evidence regarding the
359 induction of plasticity cascades, the expression of immediate early genes, as well as the
360 timeframes involved in LTP and LTD at the IC (Rosenblum et al., 1997; Hanamori et al., 1998;
361 Jones et al., 1999; Escobar and Bermúdez-Rattoni, 2000), the five treatment groups were
362 sacrificed 1 hour following taste consumption. Even though changes in activity can be observed
363 within seconds to minutes, depending on their novelty, salience and valence (Barot et al., 2008;
364 Lavi et al., 2018; Wu et al., 2020), sensory experiences can modulate the function of IC neurons
365 for hours (Juárez-Muñoz et al., 2017; Rodríguez-Durán et al., 2017; Haley et al., 2020; Kayyal et
366 al., 2021; Yiannakas et al., 2021). We had previously identified a CaMKII-dependent short-term
367 memory trace at the IC that last for the first 3 hours following taste experiences, regardless of
368 their valence (Adaikkan and Rosenblum, 2015). To address whether similar time-dependency of
369 the physiological correlations engaged by the IC during novel taste learning, a 6th group was
370 sacrificed 4 hours following novel saccharin exposure (Figure 1 – Saccharin 1x (4hrs)).

371 Daily water intake prior to the final taste exposure and the acquisition of electrophysiological

372 data was not different among the five groups that underwent water restriction (Figure 1B, One-
373 way ANOVA, $p=0.4424$, $F=0.9766$, $R^2=0.1634$). However, excitability in response to
374 incremental depolarizing currents was significantly different between the six groups (Figure 1D
375 – Two-way ANOVA, $p<0.0001$, $F(8,880)=1269$). Exposure to saccharin for the first time (i.e.,
376 novel appetitive), at the 1-hour time-point, resulted in enhanced excitability on the aIC-BLA
377 projection compared to all other groups (Figure 1D, see Table 1). Conversely, fAHP (Figure 1H;
378 One-way ANOVA, $p<0.0001$, $F=8.380$, $R^2=0.2758$) in the Quinine 1x group was
379 increased compared to all other groups, in contrast to Saccharin 1x where it was most suppressed
380 (see Table 1). In fact, fAHP in the Saccharin groups recorded at 1hr ($p<0.0001$, $z=5.150$) or
381 4hours ($p=0.0099$, $z=3.406$) following novel taste consumption was suppressed compared to
382 innately aversive Quinine 1x (Figure 1H). Even though fAHP in the Saccharin 1x group was
383 suppressed compared to both the Cage control ($p=0.0136$, $z=3.318$) and Water ($p=0.0177$, z
384 $=3.243$) groups, this was not the case for the Saccharin 1x (4hr) group ($p>0.9999$ for both – see
385 Table 1). Importantly, fAHP (Figure 1H) was nearly identical in treatment groups where the
386 tastant could be deemed as highly familiar and safe, such as the Cage control group (that did not
387 undergo water restriction), as well as animals in the Water or Saccharin 5x groups (that had
388 undergone water restriction).

389 Significant differences in terms of τ (Figure 1J; Kruskal-Wallis test, $p=0.0005$, Kruskal-Wallis
390 statistic=21.91), were only observed between the Cage control and Saccharin 1x (4hrs) groups
391 ($p=0.0040$, $z=3.647$), as well as the Saccharin 1x and Saccharin 1x (4hrs) groups ($p=0.0029$,
392 $z=3.725$). On the other hand, significant differences in AP half-width (Figure 1I; Kruskal-Wallis
393 test; $p=0.0125$, Kruskal-Wallis statistic=14.54) were only observed between the Saccharin 1x
394 (4hrs) compared to Saccharin 1x ($p=0.0065$, $z=3.519$) groups (see Table 1).

395 These results demonstrate that in the context of taste novelty, innately appetitive saccharin drove
396 increases in excitability and decreases in fAHP of LIV-VI aIC-BLA projecting neurons,
397 compared to innately aversive quinine (Figure 1D, H). Compared to the Cage control and Water
398 groups, fAHP on the projection was significantly enhanced by innately aversive quinine and was
399 suppressed by innately appetitive novel saccharin (Figure 1H). However, the effect of appetitive
400 taste novelty on firing frequency was time-dependent, as it was observed at 1hr, but not 4hrs
401 following novel taste exposure (Figure 1D). Furthermore, following familiarity acquisition for
402 saccharin (Saccharin 5x), excitability was suppressed compared to Saccharin 1x, matching the
403 Cage control, Water, and Quinine 1x groups (Figure 1D). This led us to consider whether
404 increased excitability is not related to taste identity or palatability (Wang et al., 2018), but the
405 perceived salience of taste experiences, which encompasses both novelty and valence (Ventura et
406 al., 2007; Kargl et al., 2020). Previous studies have suggested that the induction of plasticity
407 signaling cascades and IEGs in pyramidal neurons of the aIC (commonly used as surrogates for
408 changes in excitability), is a crucial step for the association of taste and visceral information
409 during CTA learning (Adaikkan and Rosenblum, 2015; Soto et al., 2017; Wu et al., 2020).
410 Activation of the aIC-BLA projection is indeed necessary for the expression of neophobia
411 towards saccharin (Kayyal et al., 2021), as well as for CTA learning and retrieval (Kayyal et al.,
412 2019). Yet, its chemogenetic inhibition does not affect the attenuation of neophobia, nor the
413 expression of aversion towards innately aversive quinine (Kayyal et al., 2019). Furthermore,
414 aversive taste memory retrieval necessitates increases in pre-synaptic inhibitory input on the
415 projection (Yiannakas et al., 2021). Bearing this in mind, we hypothesized that increases in
416 excitability on the projection could be indicative of a labile state of the taste trace at the aIC,
417 which manifests when taste cues are not (yet) highly predictive of the visceral outcome of the

418 sensory experience (Bekisz et al., 2010; Galliano et al., 2021). In such a scenario, taste memory
419 retrieval following strong single-trial aversive learning would be expected to result in decreased
420 excitability compared to control animals. To assess this hypothesis, we next examined intrinsic
421 excitability in mice retrieving an appetitive (Saccharin 2x, CTA retrieval control) or learned
422 aversive memory (CTA retrieval) for saccharin.

423

424 Learned aversive taste memory retrieval suppresses the excitability of LIV-VI aIC-BLA
425 projecting neurons

426 Following recovery from rAAV injection, mice in the CTA retrieval group underwent water
427 restriction and CTA conditioning for 0.5% saccharin (see Methods, Figure 2A).
428 Electrophysiological recordings were obtained from aIC-BLA neurons 3 days later, 1 hour
429 following retrieval (n=8 animals, 27 cells). Mice in the Saccharin 2x group on the other hand,
430 were familiarized with saccharin without conditioning, and recordings were obtained within the
431 same period, following retrieval (n=5 animals, 20 cells). Through this approach we aimed to
432 examine the hypothesis that like innately aversive and highly familiar appetitive responses
433 (Figure 1), learned aversive taste memory retrieval would be correlated with suppression of the
434 intrinsic excitability on the projection.

435 As expected, CTA retrieval mice, exhibited suppressed consumption of the conditioned tastant
436 compared to control animals that were only familiarized with saccharin (Figure 2B, Mann-
437 Whitney test, $p=0.0085$; Sum of ranks: 52.50, 38.50; Mann-Whitney $U =2.500$). Intrinsic
438 excitability in LIV-VI aIC-BLA projecting neurons was increased in response to depolarizing
439 current injections (Figure 2D; $p<0.0001$, $F(8, 360) =483.3$), and was significantly different

440 between the two treatments ($p=0.0014$, $F(1, 45) = 11.60$). Excitability was enhanced in the
441 Saccharin 2x group compared to CTA retrieval, while a significant interaction was identified
442 between the treatment and current injection factors ($p < 0.0001$, $F(8, 360) = 9.398$). Fast AHP
443 (fAHP) on LIV-VI aIC-BLA projecting neurons tended to be increased in the CTA retrieval
444 group (see Table 1), however differences compared to Saccharin 2x failed to reach significance
445 (Unpaired t-test; $p=0.0527$, $t=1.990$, $df=45$). Conversely, AP amplitude in the Saccharin 2x group
446 was significantly decreased compared to CTA retrieval (Figure 2G; Unpaired t-test; $p=0.0002$,
447 $t=3.983$, $df=45$). In addition, the CTA retrieval group exhibited significantly decreased IR
448 (Figure 2H; Unpaired t-test; $p=0.0036$, $t=3.072$, $df=45$) and significantly enhanced SAG ratio
449 (Figure 2I; Unpaired t-test; $p=0.0037$, $t=3.060$, $df=45$), compared to Saccharin 2x. In accord with
450 our hypothesis, excitability on LIV-VI aIC-BLA projecting neurons was suppressed by aversive
451 taste memory retrieval. We have previously shown that compared to CTA retrieval and
452 reinstatement, appetitive memory retrieval and extinction were associated with (a) an
453 enhancement of IEG induction (c-fos and Npas4) at the aIC, and (b) decreased frequency of pre-
454 synaptic inhibition on the aIC-BLA (Yiannakas et al., 2021). In accord, other published work
455 investigating the induction of IEG in the rodent IC, found that consistent with a reduction in
456 spiking activity (Grossman et al., 2008), the induction of c-fos at the IC was suppressed by
457 aversive taste memory retrieval (Haley et al., 2020). Earlier studies have also reported increases
458 in c-fos following the extinction of cyclosporine A-induced CTA (Hadamitzky et al., 2015). We
459 thus hypothesized that if excitability in these cells serves as key node for a change in valence
460 prediction, extinction - which constitutes a form of appetitive re-learning, would be associated
461 with enhanced excitability compared to CTA retrieval and reinstatement (Berman, 2003; Suzuki
462 et al., 2004; Morrison et al., 2016; Slouzkey and Maroun, 2016). In addition, through these

463 extinction and reinstatement studies, we were able to examine the real-life relevance of these
464 changes on intrinsic excitability, in a context where behavioral performance reflects the balance
465 between contrasting memories and the availability of retrieval cues (Figure 3).

466

467 The predictability of the valence arising from taste experiences determines the profile of
468 intrinsic properties of LIV-VI aIC-BLA projecting neurons

469 Using similar approaches, electrophysiological recordings were obtained from LIV-VI aIC-BLA
470 projecting neurons from mice having undergone unreinforced CTA extinction (Extinction; n=5,
471 14 cells), or US-mediated CTA reinstatement (Reinstatement; n=3 animals, 15 cells).

472 Behaviorally, the two groups of animals were similar in terms of their aversion profile over 9
473 unreinforced extinction sessions (Figure 3B; 2-way ANOVA; Extinction: $p < 0.0001$, $F(8, 54)$
474 $= 13.44$; Treatment: $p = 0.0681$, $F(1, 54) = 3.466$; Interaction: $p = 0.9697$, $F(8, 54) = 0.2803$). As

475 expected, saccharin consumption during the test day in the Reinstatement group was decreased
476 compared to Extinction (Figure 3C; Mann-Whitney test; $p = 0.0179$; Sum of ranks: 30, 6; Mann-
477 Whitney $U = 0$). Consistent with our findings in Figure 2, aversive taste memory retrieval in the

478 Reinstatement group was associated with suppressed excitability compared to the Extinction
479 group (Figure 3E; 2-way ANOVA, Current injection: $p < 0.0001$, $F(8, 216) = 370.1$; Treatment:
480 $p = 0.0297$, $F(1, 27) = 5.291$; Interaction: $p < 0.0001$, $F(8, 216) = 10.30$). CTA Reinstatement was

481 also associated with increases in the AP threshold (Figure 3F; Unpaired t-test: $p = 0.0076$, t
482 $= 2.887$, $df = 27$) and τ (Figure 3G; Unpaired t-test: $p = 0.0153$, $t = 2.589$, $df = 27$) compared to
483 Extinction.

484 Unlike animals that underwent familiarization with the tastant without conditioning (Figure 1),

485 excitability on the projection in the Extinction group was not suppressed by familiarization
486 (Figure 3). Conversely, even though the intrinsic mechanisms employed would appear to differ,
487 aversive taste memory retrieval regardless of prior experience, was associated with baseline
488 excitability of the aIC-BLA projection (Figure 3). Our findings in this section (Figure 3),
489 revealed that during taste memory retrieval, excitability on the projection is not solely dependent
490 on the relevant novelty or appetitive nature of tastants, and does not subserve the persistence of
491 CTA memories (Figure 2). Instead, excitability on the aIC-BLA projection is indeed shaped by
492 prior experience but is best predicted by the probability for further aversive (re)learning.

493 Next, to distinguish between intrinsic properties changes that reproducibly reflect taste identity,
494 familiarity, and valence over the course of time and experience, we compared the profile of
495 intrinsic properties across pairs of behavioral groups in which the currently perceived novelty, as
496 well as innate or learned valence associated with taste was notably different. Through this
497 comparison, we were led to conclude that excitability on aIC-BLA projecting neurons is driven
498 by taste stimuli of positive valence, however this effect is dependent on subjective experience
499 and the possibility for further associative learning (Figure 4A). Excitability on aIC-BLA
500 projecting neurons in the treatment groups where the tastant was perceived as appetitive
501 (Saccharin 1x, Saccharin 2x and Extinction), was closely matched, and was significantly
502 enhanced compared to the innately or learned aversive (Quinine 1x, CTA retrieval and
503 Reinstatement) groups (Figure 4A; Two-way ANOVA; Current injection: $p < 0.0001$, $F(5, 872)$
504 $= 1218$; Treatment: $p = 0.0014$, $F(5, 109) = 4.281$; Interaction: $p < 0.0001$, $F(40, 872) = 4.978$). As
505 previously identified in Figure 1H, fAHP reflected the innate aversive nature of the tastant, being
506 increased in the Quinine 1x group compared to all other groups (Figure 4B; One-way ANOVA;
507 $F = 10.65$, $p < 0.0001$, $R^2 = 0.3283$, see Table 1). Significant differences in IR (Figure 4C;

508 One-way ANOVA; $F = 2.775$, $p=0.0213$, $R^2=0.1129$) and SAG ratio (Figure 4D; One-
509 way ANOVA; $F = 2.610$, $p=0.0286$, $R^2=0.1069$) were only observed between the CTA
510 retrieval and Saccharin 2x groups. AP amplitude (Figure 4E; One-way ANOVA, $p=0.0054$,
511 $F=3.526$, $R^2=0.1392$) in the Saccharin 2x group was suppressed compared to both CTA
512 retrieval ($p=0.0129$, $q=4.768$, $df=109$) and Quinine 1x ($p=0.0087$, $q=4.944$, $df=109$). Conversely,
513 the Extinction and Reinstatement groups, where familiarity with the tastant was the highest,
514 exhibited increased AP half-width compared to all other groups (Figure 4F; One-way ANOVA,
515 Kruskal-Wallis test; $p=0.0002$; Kruskal-Wallis statistic, 24.03). Significant differences in terms
516 of τ (Figure 4G; One-way ANOVA, $p=0.0047$, $F = 3.606$) were only observed in comparing the
517 Saccharin 1x and Reinstatement groups ($p=0.0022$, $q=5.525$, $df=109$). Hence, neuronal
518 excitability is indeed a feature associated with predictive power to modulate taste valence,
519 however it does not fully reflect the breadth of intrinsic property changes among the different
520 behavioral groups.

521

522 The predictability of taste valence intrinsic is primarily reflected on the excitability of
523 burst-spiking, but not regular-spiking LIV-VI aIC-BLA projecting neurons

524 Our initial analysis of individual intrinsic properties (Figures 1-3) highlighted that excitability is
525 enhanced following appetitive experiences in which the internal representation is still labile and
526 is associated with the possibility for further aversive learning (novelty or extinction). Conversely,
527 following extensive familiarization, aversive conditioning, or reinstatement, whereby taste
528 exposure leads to memory retrieval of specific valence, excitability on LIV-VI aIC-BLA
529 projecting neurons was similar to baseline (Figures 1 and 4). While the precise mechanism
530 through which sensory input is encoded at the cortex (and other key regions), is still a matter of

531 ongoing research, studies indicate that bursting in cortical layer V pyramidal neurons can encode
532 oscillating currents into a pattern that can be reliably transmitted to distant post-synaptic
533 terminals (Kepecs and Lisman, 2003; Samengo et al., 2013; Zeldenrust et al., 2018). Spike burst
534 is defined as the occurrence of three or more spikes from a single neurons with <8ms intervals
535 (Ranck, 1973; Connors et al., 1982). In brain slices from naïve mice, half of the neurons of a
536 given structure exhibit burst firing, while the distribution of burst-spiking (BS) to regular-spiking
537 (RS) neurons, changes along the anterior-posterior axis of the subiculum (Staff et al., 2000;
538 Jarsky et al., 2008). Importantly, the two cell types fine-tune the output of brain structures by
539 virtue of differences in synaptic plasticity, as well as intrinsic excitability mechanisms (Graves et
540 al., 2012; Song et al., 2012). Furthermore, there are changes in the ratio of BS:RS neurons in
541 individual brain structures, as well as differences in the recruitment of signaling events, ion
542 channels and metabotropic receptors among the two cell types (Wozny et al., 2008; Shor et al.,
543 2009). Correspondingly, complex region and task-specific rules govern the molecular and
544 electrophysiological mechanisms through which information encoding and retrieval takes place
545 in the two cell types (Dunn et al., 2018; Dunn and Kaczorowski, 2019). Little is currently known
546 regarding the influence of cell identity in the repertoire of plasticity mechanisms employed by
547 the IC to facilitate taste-guided behaviors (Maffei et al., 2012; Haley and Maffei, 2018).

548 Our post-hoc spike sorting analysis allowed us to distinguish between BS and RS LIV-VI aIC-
549 BLA projecting neurons, and thus their relative contribution to behaviorally driven changes in
550 the suit of intrinsic properties (Extended Figures 1-3, 2-1 and 3-1). Through this comparison, we
551 uncovered that Saccharin 1x differed to other groups in terms of excitability and fAHP in BS
552 LIV-VI aIC-BLA neurons (Extended Figure 1-3), while no such changes were observed in RS
553 neurons (see Summary of RS intrinsic properties table no.4). Similarly, excitability in the

554 Saccharin 2x group was significantly enhanced compared to CTA retrieval in BS-, but not in RS
555 LIV-VI aIC-BLA neurons (Extended Figure 2-1A, F). Significant differences in IR, SAG ratio
556 and AP amplitude between CTA retrieval and Saccharin 2x were primarily driven by BS LIV-VI
557 aIC-BLA neurons (Extended Figure 2-1B-D, G-I). Conversely, significant differences in AP half-
558 width between the aversive and appetitive memory retrieval groups were only observed in RS
559 neurons (Extended Figure 2-1J). Correspondingly, excitability in the Extinction group was
560 enhanced compared to Reinstatement in BS-, and not RS LIV-VI aIC-BLA neurons (Extended
561 Figure 3-1A, H). Indeed, excitability on BS LIV-VI aIC-BLA neurons following extinction and
562 reinstatement, reflected the subjective predictability of taste memory retrieval, being high
563 following extinction compared to reinstatement (Extended Figure 3-1). However, this effect was
564 mediated through alternative mechanisms compared to single-trial learning and memory retrieval
565 (Extended Figure 1-3, 2-1, 3-1). Significant differences between the Extinction and
566 Reinstatement groups, were observed in terms of the sAHP, AP threshold, SAG ratio and τ in BS
567 but not in RS LIV-VI aIC-BLA neurons (Extended Figure 3-1B-F).

568 Encouraged by these findings, we focused on the Saccharin 1x, Saccharin 2x, Saccharin 5x, CTA
569 Retrieval, Extinction and Reinstatement groups, as to isolate the contribution of BS LIV-VI aIC-
570 BLA neurons in encoding the subjective predictability of taste experience during taste learning,
571 re-learning, and memory retrieval (Figure 5). Consistent with studies in the hippocampus
572 (Graves et al., 2016), we found that the percentage of BS LIV-VI aIC-BLA projecting neurons in
573 the sampled population was highest in the context of novel taste learning (Extended Figure 1-2B:
574 Saccharin 1x, 85%), and subsided following progressive familiarization (Extended Figure 1-2B;
575 Saccharin 2x, 65%, Mann-Whitney test: $p=0.0562$; Sum of ranks: 303.5, 161.5; Mann-Whitney
576 $U=70.50$; Saccharin 5x, 55.56%, Mann-Whitney test: $p=0.0034$; Sum of ranks: 291, 87; Mann-

577 Whitney U =32;). Interestingly, animals retrieving CTA, exhibited the lowest proportion of BS
578 neurons among the six treatments (Extended Figure 1-2B; CTA retrieval, 44.44% BS), and
579 significant differences were observed compared to control animals (Extended Figure 1-2B;
580 Saccharin 2x, 65% BS; Mann-Whitney test: $p=0.0102$; Sum of ranks: 257, 208; Mann-Whitney
581 U =55). Thus, the ratio of BS:RS LIV-VI aIC-BLA projecting neurons was plastic in relation to
582 experience and was highest in response to appetitive novelty – in accord with studies
583 investigating the intrinsic excitability of subiculum output neurons in relation to contextual
584 novelty and valence encoding (Dunn et al., 2018). Indeed, the ratio of BS:RS LIV-VI aIC-BLA
585 neurons was progressively suppressed by familiarity acquisition (Saccharin 1x > 2x > 5x), as well
586 as following aversive taste memory recall (CTA retrieval), compared to both appetitive learning
587 (Extended Figure 1-2B; Saccharin 1x, Mann-Whitney test: $p<0.0001$; Sum of ranks: 407, 188;
588 Mann-Whitney U =35) and re-learning (Extended Figure 1-2B; Extinction, Mann-Whitney test:
589 $p=0.0007$; Sum of ranks: 182, 224; Mann-Whitney U =29). However, our comparison failed to
590 account for the influence of complex experiences over time, as differences between Extinction
591 and Reinstatement failed to reach significance (Extended Figure 1-2B; Mann-Whitney test:
592 $p=0.3870$, Sum of ranks: 133.5, 97.50, Mann-Whitney U =42.50), while perplexingly, the ratio
593 of BS:RS aIC-BLA neurons in these groups was differentially increased compared to Saccharin
594 5x (Extended Figure 1-2B; Extinction, Mann-Whitney test: $p=0.0300$; Sum of ranks: 81, 150;
595 Mann-Whitney U =26; Reinstatement, Mann-Whitney test: $p=0.3498$; Sum of ranks: 90, 120;
596 Mann-Whitney U =35;), but not Saccharin 2x (Extended Figure 1-2B; Extinction, Mann-
597 Whitney test: $p=0.2397$; Sum of ranks: 143.5, 156.5; Mann-Whitney U =52.50; Reinstatement,
598 Mann-Whitney test: $p>0.9999$; Sum of ranks: 153.50, 122.5; Mann-Whitney U =62.50). No
599 further statistics were performed in intrinsic properties of aIC-BLA regular spiking neurons

600 representing (Figure 1 and Figure 3), because of the small sample size.

601 Changes in the intrinsic properties of neuronal ensembles have recently been suggested to
602 contribute to homeostatic mechanisms integrating both cellular and synaptic information (Wu et
603 al., 2021). In our current study, we randomly sampled from neuroanatomically defined LIV-VI
604 aIC-BLA projecting neurons, and even following spike sorting (Extended Figures 1-2), the
605 probability of recording from engram cells (10% of neurons within a region) would be extremely
606 low (Tonegawa et al., 2015). Importantly, the correlative nature does not exclude the possibility
607 that these changes are the consequence of representational drift (Driscoll et al., 2017). We thus
608 set out to examine the hypothesis that applying linear dimension reduction method on the
609 complement of intrinsic properties recorded in BS LIV-VI aIC-BLA neurons would allow us to
610 distinguish between taste experiences that differ in terms of their perceived predictability (or the
611 associated probability for further aversive learning).

612

613 Principal component analysis of the profile of intrinsic properties in BS LIV-VI aIC-BLA
614 projecting neurons separates treatment groups in relation to the perceived predictability
615 of taste valence for saccharin

616 We assigned six of our treatment groups into highly predictive scenarios (Saccharin 5x, CTA
617 retrieval and Reinstatement), and low predictive scenarios (Saccharin 1x, Saccharin 2x,
618 Extinction). We used parallel analysis to select the components across the complement of
619 intrinsic properties in each treatment group, with the first three principal components (PC1-3)
620 explaining 30.84%, 17.88%, and 13.75% of the total variance, respectively, and 62.47% of the
621 variance, collectively (Figure 5-2). PC1 (Figure 5B, Extended Figure 5-2) was characterized by

622 strong negative loadings for Rheobase (-0.88304), sAHP (-0.85985) and mAHP (-0.82421),
623 while a positive correlation was identified for IR (0.694764). The direction of PC2 (Figure 5B,
624 Extended Figure 5-2) was positively correlated with fAHP (0.682681) and AP halfwidth
625 (0.614103) and was negatively correlated with Excitability at 350pA (-0.69587). PC3 (Figure 5B,
626 Extended Figure 5-2) positively correlated with SAG ratio (0.889949) and RMP (0.682681),
627 whereas a significant negative correlation with mAHP (-0.6095) was also identified. Unlike
628 aversive or appetitive taste memory retrieval (i.e., highly predictive), appetitive novelty or
629 extinction learning (i.e., low predictive), was associated with increased input resistance, faster
630 action potential generation and suppressed afterhyperpolarization on BS aIC-BLA neurons
631 (Figure 5). Importantly, PCA of the intrinsic properties of LIV-VI aIC-BLA projecting neurons
632 regardless of cell type (BS and RS together, Extended Figure 5-1), failed to segregate the two
633 groups of treatments. This cell-type specific profile of intrinsic properties could provide the
634 framework through which BS LIV-VI aIC-BLA projecting neurons are able to inspect the
635 gastrointestinal consequences associated with tastants over prolonged timescales, when these
636 consequences are not accurately predicted by sensory experience or memory retrieval alone
637 (Adaikkan and Rosenblum, 2015; Lavi et al., 2018; Kayyal et al., 2019).

638

639 Discussion

640 Learning and memory are subserved by plasticity in both synapse strength and neuronal intrinsic
641 properties (Citri and Malenka, 2008; Sehgal et al., 2013). While Hebbian rules can explain asso-
642 ciative learning paradigms where seconds separate the CS and US (Krabbe et al., 2018), addi-
643 tional cellular-level mechanisms are needed to explain how learning operates in paradigms where

644 the time between CS and US extends to hours (Adaikkan and Rosenblum, 2015; Wu et al.,
645 2021). In this study, we demonstrate that following taste experiences, taste percept and prior ex-
646 perience are integrated in the intrinsic properties of the aIC in a time-dependent and cell-type
647 specific manner. We further show that regardless of the identity or prior history associated with
648 taste, the intrinsic properties of BS LIV-VI aIC-BLA projecting neurons encodes the perceived
649 confidence of taste valence attribution.

650 We focused on the aIC-BLA projection; a circuit causally involved in the acquisition and retriev-
651 al of CTA memories (Kayyal et al., 2019, 2021). (Kayyal et al., 2019, 2021). We examined the
652 hypothesis that excitability in aIC-BLA neurons can serve as a taste valence updating mechanism
653 enabling the prolonged ISI between CS and US in CTA learning (Adaikkan and Rosenblum,
654 2015), and/or contributes to anticipatory valence attribution (Barrett and Simmons, 2015). Our
655 basic proposition diverged from Hebb's famous postulate that cells with increased excitability
656 over hours can potentially wire together with cells conveying incoming modified valence infor-
657 mation (Hebb, 1961).

658 The confidence with which taste valence is encoded is the product of the subjectively perceived-
659 (a) appetitive or aversive nature of tastants and (b) novelty or familiarity associated with tastants
660 (Russell, 1980; Kahnt and Tobler, 2017). We first examined each axis separately and later in tan-
661 dem as to better simulate real-life scenarios. We measured the intrinsic properties of aIC-BLA
662 neurons 1 hour following taste experience – a previously established suitable time point (Jones et
663 al., 1999; Haley et al., 2020).

664 To dissociate novelty-related changes from those involving hydration, taste identity and familiar-
665 ity; we compared the intrinsic properties of aIC-BLA neurons following Water – a neutral and
666 familiar tastant, Saccharin – an innately appetitive tastant, in the context of novelty (1x) or famil-

667 iarity (5x), and Quinine – an innately aversive novel tastant (Figure 1). Excitability was high fol-
668 lowing novel saccharin exposure, but not in response to Quinine (Figure 1D). Indeed, concerted
669 activity at the aIC and BLA encodes the presence, identity and palatability of taste experiences
670 within the 2 seconds preceding swallowing (Katz et al., 2001; Grossman et al., 2008; Fontanini
671 et al., 2009). Palatability can be enhanced as a function of experience (Austen et al., 2016), but
672 can also be suppressed by sensory satiety and alliesthenia (Rolls et al., 1981; Yeomans, 1998;
673 Siemian et al., 2021). However, excitability on the projection was enhanced in response to novel-
674 ty and was suppressed following familiarization (Figure 1). Further inconsistent with palatability
675 encoding; changes in excitability captured 1 hour following novel saccharin exposure subsided 4
676 hours later (Figure 1), while excitability remained plastic even following longer periods of water
677 restriction, that could be considered monotonous (Figure 5). Deciphering whether and how aIC-
678 BLA neurons contribute to palatability processing would require *in vivo* recordings to capture
679 taste-evoked changes, within timescales that are beyond the scope and means of our current
680 study (Vincis and Fontanini, 2016).

681 The correlation identified between excitability and innate current taste valence, encouraged us to
682 examine the predictability of future outcomes following aversive taste memory retrieval. Bearing
683 in mind our previous findings using transcription-dependent activity markers at the aIC (Yian-
684 nakas et al., 2021), we hypothesized that aversive taste memory retrieval (CTA retrieval or Rein-
685 statement), would be associated with suppressed excitability compared to stimulus- and famili-
686 arity-matched controls (Saccharin 2x and Extinction). Indeed, excitability on aIC-BLA projecting
687 neurons following CTA retrieval was suppressed compared to Saccharin 2x (Figure 2B), while
688 Reinstatement, was also associated with decreased excitability compared to Extinction (Figure
689 3E). Hence, regardless of the complexity of taste memory retrieval, excitability in aIC-BLA neu-

690 rons was best expected by the subjective predictability of taste valence - increasing in response
691 to innately appetitive taste experiences in which the perceived possibility for avoidance learning
692 was high/taste valence predictability was low (Figure 4). Conversely, when the subjective confi-
693 dence with which taste valence was predicted was high, excitability on the projection remained
694 unchanged (Figures 1, 4).

695 Innately and learned aversive tastants were both associated with suppressed excitability on aIC-
696 BLA projecting neurons compared to appetitive controls, however these effects were mediated
697 through alternative mechanisms (Figures 2-4). Quinine increased fAHP on the projection com-
698 pared to saccharin, regardless of familiarity or perceived valence (Figures 1 and 4). Post-spike
699 after-hyperpolarization (AHP) has a key function in transducing the summed result of processed
700 synaptic input, directly impacting neuronal excitability in relation to both learning and aging (Oh
701 and Disterhoft, 2020). In pyramidal cells of the hippocampus and cortex, differences in fAHP are
702 mediated by the Ca^{2+} and voltage-dependent BK currents that promote repolarization at the be-
703 ginning APs trains (Shao et al., 1999). Interestingly, studies in the prefrontal cortex (PFC), have
704 shown that fear conditioning decreases excitability, whereas extinction training enhances excita-
705 bility and decreases medium- and slow AHP (Santini et al., 2008; Maglio et al., 2021). At the IC,
706 chronic ethanol consumption has shown to decrease excitability and to increase AHP (Luo et al.,
707 2021). Conversely, oxytocin-dependent signaling at the IC has been shown to promote social af-
708 fective behaviors, via increases in excitability and decreases in sAHP (Rogers-Carter et al.,
709 2018). Further studies would be necessary to fully address this, but our findings could indicate
710 that enhanced fAHP is induced by innately aversive tastants or quinine specifically.

711 Unlike Quinine, CTA memory retrieval, was associated with increased AP amplitude and SAG
712 ratio, as well as decreased IR in BS LIV-VI aIC-BLA projecting neurons, compared to control

713 animals (Figure 2, Extended Figure 2-1). On the other hand, the suppressed excitability in the
714 Reinstatement group compared to Extinction was characterized by decreased AP threshold, in-
715 creased τ , and decreased sAHP (Figures 3, 4, Extended Figure 3-1). The hyperpolarization-
716 activated, cyclic nucleotide-gated current (I_h) regulates membrane depolarization following hy-
717 perpolarization (Hogan and Poroli, 2008; Shah, 2014). The opening of HCN channels generates
718 an inward current, that modulates AHP, RMP and IR in cortical pyramidal and PV interneurons
719 (Yang et al., 2018). However, conductance through I_h channels, regulates synaptic integration at
720 the soma of pyramidal neurons, by suppressing excitability, decreasing IR, and increasing τ (Ho-
721 gan and Poroli, 2008). Evidence indicates that this dichotomous impact of HCN channels on neu-
722 ronal excitability, is mediated by A-type K channels at the dendrites (Mishra and Narayanan,
723 2015), and M-type channels at the soma (Hu et al., 2007). Notably, AP half-width was signifi-
724 cantly increased in the Extinction and Reinstatement groups that had undergone extinction train-
725 ing, compared to all other saccharin-treated groups (Figure 4F). Mechanistically, this effect could
726 reflect changes in the distribution and/or the properties of voltage- or calcium-gated ion channels
727 (Faber and Sah, 2002; Grubb and Burrone, 2010; Kuba et al., 2010). Such broadening of spike
728 width has also been reported in infralimbic PFC neurons projecting to the amygdala in response
729 to extinction training (Senn et al., 2014). PV-dependent restriction of excitability and burst fir-
730 ing, is instrumental in experience-dependent plasticity in the amygdala (Morrison et al., 2016),
731 the hippocampus (Donato et al., 2013; Xia et al., 2017) and visual cortex (Yazaki-Sugiyama et
732 al., 2009; Kuhlman et al., 2013). Conversely, in the striatum, PV interneurons restrict bursting,
733 calcium influx, and synaptic plasticity to appropriate temporal windows that facilitate learning,
734 but not retrieval (Owen et al., 2018). Elegant recent studies report that rapid eye movement sleep
735 is associated with a PV-dependent somatodendritic decoupling in pyramidal neurons of the PFC

736 (Aime et al., 2022). At the IC, the maturation of GABAergic PV circuits is key for multisensory
737 integration and pruning of cross-modal input to coordinate the detection of relevant information
738 (Gogolla et al., 2014). Activation of IC PV disrupts the expression of taste-guided goal-directed
739 behavior (Vincis et al., 2020), and enhances taste-guided aversive responses (Yiannakas et al.,
740 2021). Our findings could be indicative of a prediction-dependent decoupling mechanism at the
741 IC, whereby the restriction of bursting activity in LIV-VI aIC-BLA neurons impinges on innate
742 drives towards the tastant and further learning, depending on prior experience.

743 We further probed our results and hypotheses using PCA and attempted to segregate behaviors
744 based on the perceived ability of the CS to predict the consequences of sensory experience, and
745 the probability for further learning (Figure 5). We focused on BS LIV-VI aIC-BLA projecting
746 neurons since bursting has been implicated in coincidence detection by deep-layer neurons
747 (Boudewijns et al., 2013; Shai et al., 2015), as well as the encoding of novelty and valence relat-
748 ing to different modalities (Song et al., 2015; Dunn et al., 2018; Yousuf et al., 2019). Our PCA of
749 intrinsic properties in BS LIV-VI aIC-BLA projecting neurons demonstrated that distinct plastici-
750 ty rules are at play depending on the balance between the probability for associative learning and
751 the certainty with which taste predicts the valence of experience during retrieval (Figure 6). We
752 propose that increased excitability and reduced fAHP on BS LIV-VI aIC-BLA projecting neu-
753 rons might represent a transient neuronal state in the absence of adequate predictive cues for the
754 outcome of taste experiences (Adaikkan and Rosenblum, 2015).

755 The IC has long been considered crucial for interoception, which is increasingly understood to be
756 supported by distinct direct or indirect functional bidirectional connectivity. Indeed, interoceptive
757 inputs relating to the processing, or anticipation of physiological states of hydration and satiety
758 manifest at the pIC (Livneh et al., 2017, 2020; Livneh and Andermann, 2021). However, this is

759 rarely the case when it comes to physiological hydration or satiety inputs and the aIC, that has is
760 primarily involved in interoceptive processes in the context food poisoning or CTA (Chen et al.,
761 2020; Wu et al., 2020). As other studies currently in press demonstrate, hydration correlates and
762 requires suppressed activity in aIC-BLA and increases in pIC-BLA CB1 receptor-expressing
763 neurons (Zhao et al., 2020; Nicolas et al., 2022). Under uncertain conditions that are associated
764 with greater potential significance, recruitment of the aIC is thought to contribute to attention,
765 effort, and accurate processing (Lovero et al., 2009), as to identify better response options
766 (Preuschoff et al., 2008). In agreement with earlier computational models of the cortical connec-
767 tivity (Mumford, 1991, 1992), recent work indicates that the aIC facilitates prediction-related
768 encoding driven by hedonics, rather than homeostatic needs (Darevsky et al., 2019; Price et al.,
769 2019; Darevsky and Hopf, 2020). Our results, propose a cellular framework for such an emo-
770 tional predictive function at the aIC. Future studies will further explore whether and how the in-
771 terplay between such distinct mechanisms at the aIC, enables its complex role in learning,
772 memory, and decision-making.

773

774 Conflict of interest statement

775 Authors report no conflict of interest.

776

777 Data availability

778 All data generated or analyzed during this study are included in the manuscript and supporting
779 files. Source data files have been provided for all figures.

780

781 Author contributions

782 SKC and AY led the project. AY, SKC and KR designed the research. KR supervised the
783 research. SKC, AY, HK, and MK performed the research. SKC, AY, LM, RS, FC, and SS
784 analyzed the data. AY, SKC and KR drafted the paper. All authors reviewed and contributed to
785 the manuscript.

786

787 Acknowledgments

788 The authors would like to thank all current members of the Rosenblum labs for their help and
789 support, to the veterinary team headed by Barak Carmi and Corina Dollinger and technical team
790 headed by Yair Bellehsen. Graphical illustrations were created using BioRender.com.

791

792 Funding

793 This research was supported by a grant from the Israel Science Foundation (ISF); ISF 946/17 and
794 ISF 258/20 to KR.

795

796 References

- 797 Adaikkan C, Rosenblum K (2015) A molecular mechanism underlying gustatory memory trace
798 for an association in the insular cortex. *Elife* 4:1–15.
- 799 Aime M, Calcini N, Borsa M, Campelo T, Rusterholz T, Sattin A, Fellin T, Adamantidis A (2022)
800 Paradoxical somatodendritic decoupling supports cortical plasticity during REM sleep.
801 Available at: <https://www.science.org>.

- 802 Andrade R, Foehring RC, Tzingounis A v. (2012) The calcium-activated slow AHP: Cutting
803 through the Gordian Knot. *Frontiers in Cellular Neuroscience*:1–38.
- 804 Arieli E, Gerbi R, Shein-Idelson M, Moran A (2020) Temporally-precise basolateral amygdala
805 activation is required for the formation of taste memories in gustatory cortex. *Journal of*
806 *Physiology* 598.
- 807 Austen JM, Strickland JA, Sanderson DJ (2016) Memory-dependent effects on palatability in
808 mice. *Physiology and Behavior* 167.
- 809 Bachmanov AA, Reed DR, Tordoff MG, Price RA, Beauchamp GK (1996) Intake of ethanol,
810 sodium chloride, sucrose, citric acid, and quinine hydrochloride solutions by mice: A
811 genetic analysis. *Behavior Genetics* 26:563–573.
- 812 Bales MB, Schier LA, Blonde GD, Spector AC (2015) Extensive gustatory cortex lesions
813 significantly impair taste sensitivity to KCl and quinine but not to sucrose in rats. *PLoS*
814 *ONE* 10:1–25.
- 815 Barot SK, Kyono Y, Clark EW, Bernstein IL (2008) Visualizing stimulus convergence in
816 amygdala neurons during associative learning. *Proceedings of the National Academy of*
817 *Sciences* 105:20959–20963.
- 818 Barrett LF, Simmons WK (2015) Interoceptive predictions in the brain. *Nature Reviews*
819 *Neuroscience* 16:419–429.
- 820 Bekisz M, Garkun Y, Wabno J, Hess G, Wrobel A, Kossut M (2010) Increased excitability of
821 cortical neurons induced by associative learning: An ex vivo study. *European Journal of*
822 *Neuroscience* 32:1715–1725.
- 823 Berman DE (2003) Modulation of taste-induced Elk-1 activation by identified neurotransmitter
824 systems in the insular cortex of the behaving rat. *Neurobiology of Learning and Memory*
825 79:122–126.
- 826 Boudewijns ZSRM, Groen MR, Lodder B, McMaster MTB, Kalogreades L, Haan R De,
827 Narayanan RT, Meredith RM, Mansvelder HD, de Kock CPJ (2013) Layer-specific high-
828 frequency spiking in the prefrontal cortex of awake rats. *Frontiers in Cellular Neuroscience*.
- 829 Bures J, Bermudez-Rattoni F, Yamamoto T (1998) The CTA paradigm. In: *Conditioned Taste*
830 *Aversion, memory of a special kind*.
- 831 Chakraborty D, Fedorova O v., Bagrov AY, Kaphzan H (2017) Selective ligands for Na⁺/K⁺-
832 ATPase α isoforms differentially and cooperatively regulate excitability of pyramidal
833 neurons in distinct brain regions. *Neuropharmacology* 117:338–351.
- 834 Chen K, Kogan J, Fontanini A (2020) Spatially distributed representation of taste quality in the
835 gustatory insular cortex of awake behaving mice. *Current Biology*:1–10.
- 836 Chinnakkaruppan A, Wintzer ME, McHugh TJ, Rosenblum K (2014) Differential Contribution
837 of Hippocampal Subfields to Components of Associative Taste Learning. *Journal of*

- 838 Neuroscience.
- 839 Citri A, Malenka RC (2008) Synaptic plasticity: Multiple forms, functions, and mechanisms.
840 *Neuropsychopharmacology* 33:18–41.
- 841 Connors BW, Gutnick MJ, Prince DA (1982) Electrophysiological properties of neocortical
842 neurons in vitro. *Journal of Neurophysiology* 48:1302–1320.
- 843 Darevsky D, Gill TM, Vitale KR, Hu B, Wegner SA, Hopf FW (2019) Drinking despite
844 adversity: behavioral evidence for a head down and push strategy of conflict-resistant
845 alcohol drinking in rats. *Addiction Biology* 24:426–437.
- 846 Darevsky D, Hopf FW (2020) Behavioral indicators of succeeding and failing under higher-
847 challenge compulsion-like alcohol drinking in rat. *Behavioural Brain Research* 393.
- 848 Disterhoft JF, Wu WW, Ohno M (2004) Biophysical alterations of hippocampal pyramidal
849 neurons in learning, ageing and Alzheimer’s disease. *Ageing Research Reviews* 3:383–406.
- 850 Donato F, Rompani SB, Caroni P (2013) Parvalbumin-expressing basket-cell network plasticity
851 induced by experience regulates adult learning. *Nature*.
- 852 Dunn AR, Kaczorowski CC (2019) Regulation of intrinsic excitability: Roles for learning and
853 memory, aging and Alzheimer’s disease, and genetic diversity. *Neurobiology of Learning
854 and Memory* 164.
- 855 Dunn AR, Neuner SM, Ding S, Hope KA, O’Connell KMS, Kaczorowski CC (2018) Cell-type-
856 specific changes in intrinsic excitability in the subiculum following learning and exposure
857 to novel environmental contexts. *eNeuro* 5:18.2018.
- 858 Escobar ML, Bermúdez-Rattoni F (2000) Long-term potentiation in the insular cortex enhances
859 conditioned taste aversion retention. *Brain Research* 852:208–212.
- 860 Faber ESL, Sah P (2002) Physiological role of calcium-activated potassium currents in the rat
861 lateral amygdala. *Journal of Neuroscience* 22.
- 862 Fontanini A, Grossman SE, Figueroa JA, Katz DB (2009) Distinct Subtypes of Basolateral
863 Amygdala Taste Neurons Reflect Palatability and Reward. *Journal of Neuroscience*
864 29:2486–2495.
- 865 Galliano E, Hahn C, Browne LP, Villamayor PR, Tufo C, Crespo A, Grubb MS (2021) Brief
866 sensory deprivation triggers cell type-specific structural and functional plasticity in
867 olfactory bulb neurons. *Journal of Neuroscience* 41:2135–2151.
- 868 Garcia J, Kimeldorf DJ, Koelling RA (1955) Conditioned aversion to saccharin resulting from
869 exposure to gamma radiation. *Science* 122:157–158.
- 870 Gogolla N, Takesian AE, Feng G, Fagiolini M, Hensch TK (2014) Sensory integration in mouse
871 insular cortex reflects GABA circuit maturation. *Neuron* 83:894–905.
- 872 Graves AR, Moore SJ, Bloss EB, Mensh BD, Kath WL, Spruston N (2012) Hippocampal

- 873 Pyramidal Neurons Comprise Two Distinct Cell Types that Are Countermodulated by
874 Metabotropic Receptors. *Neuron* 76:776–789.
- 875 Graves AR, Moore SJ, Spruston N, Tryba AK, Kaczorowski CC (2016) Brain-derived
876 neurotrophic factor differentially modulates excitability of two classes of hippocampal
877 output neurons. *Journal of Neurophysiology* 116:466–471.
- 878 Greenhill SD, Ranson A, Fox K (2015) Hebbian and Homeostatic Plasticity Mechanisms in
879 Regular Spiking and Intrinsic Bursting Cells of Cortical Layer 5. *Neuron* 88:539–552.
- 880 Grossman SE, Fontanini A, Wieskopf JS, Katz DB (2008) Learning-related plasticity of temporal
881 coding in simultaneously recorded amygdala-cortical ensembles. *Journal of Neuroscience*
882 28:2864–2873.
- 883 Grubb MS, Burrone J (2010) Activity-dependent relocation of the axon initial segment fine-tunes
884 neuronal excitability. *Nature* 465.
- 885 Hadamitzky M, Börsche K, Engler A, Schedlowski M, Engler H (2015) Extinction of conditioned
886 taste aversion is related to the aversion strength and associated with c-fos expression in the
887 insular cortex. *Neuroscience* 303:34–41.
- 888 Haley MS, Bruno S, Fontanini A, Maffei A (2020) LTD at amygdalocortical synapses as a novel
889 mechanism for hedonic learning. *Elife*.
- 890 Haley MS, Fontanini A, Maffei A (2016) Laminar- and Target-Specific Amygdalar Inputs in Rat
891 Primary Gustatory Cortex. *The Journal of Neuroscience* 36:2623–2637.
- 892 Haley MS, Maffei A (2018) Versatility and Flexibility of Cortical Circuits. *Neuroscientist*.
- 893 Hanamori T, Kunitake T, Kato K, Kannan H (1998) Responses of neurons in the insular cortex to
894 gustatory, visceral, and nociceptive stimuli in rats. *J Neurophysiol* 79:2535–2545 Available
895 at: <http://www.ncbi.nlm.nih.gov/pubmed/9582226>.
- 896 Hebb DO (1961) Distinctive features of learning in the higher animal. *Brain mechanisms and*
897 *learning: A Symposium*:37–46.
- 898 Hogan QH, Poroli M (2008) Hyperpolarization-activated current (I_h) contributes to excitability
899 of primary sensory neurons in rats. *Brain Research* 1207:102–110.
- 900 Hu H, Vervaeke K, Storm JF (2007) M-channels (K_v7/KCNQ channels) that regulate synaptic
901 integration, excitability, and spike pattern of CA1 pyramidal cells are located in the
902 perisomatic region. *Journal of Neuroscience* 27.
- 903 Jarsky T, Mady R, Kennedy B, Spruston N (2008) Distribution of bursting neurons in the CA1
904 region and the subiculum of the rat hippocampus. *Journal of Comparative Neurology* 506.
- 905 Jones MW, French PJ, Bliss T V., Rosenblum K (1999) Molecular mechanisms of long-term
906 potentiation in the insular cortex in vivo. *J Neurosci* 19:RC36–RC36.
- 907 Juárez-Muñoz Y, Ramos-Languren LE, Escobar ML (2017) CaMKII Requirement for in Vivo

- 908 Insular Cortex LTP Maintenance and CTA Memory Persistence. *Front Pharmacol*.
- 909 Kahnt T, Tobler PN (2017) Reward, value, and salience. In: *Decision Neuroscience: An*
910 *Integrative Perspective*, pp 109–120.
- 911 Kaphzan H, Buffington SA, Ramaraj AB, Lingrel JB, Rasband MN, Santini E, Klann E (2013)
912 Genetic reduction of the $\alpha 1$ Subunit of Na/K-ATPase corrects multiple hippocampal
913 phenotypes in angelman syndrome. *Cell Reports*.
- 914 Kargl D, Kaczanowska J, Ulonska S, Groessl F, Piszczek L, Lazovic J, Buehler K, Haubensak W
915 (2020) The amygdala instructs insular feedback for affective learning. *Elife* 9:1–36.
- 916 Katz DB, Simon SA, Nicolelis MA (2001) Dynamic and multimodal responses of gustatory
917 cortical neurons in awake rats. *J Neurosci*.
- 918 Kayyal H, Kolatt Chandran S, Yiannakas A, Gould N, Khamaisy M, Rosenblum K (2021) Insula
919 to mPFC reciprocal connectivity differentially underlies novel taste neophobic response and
920 learning. *Elife* 10 Available at: <http://www.ncbi.nlm.nih.gov/pubmed/34219650>.
- 921 Kayyal H, Yiannakas A, Kolatt Chandran S, Khamaisy M, Sharma V, Rosenblum K, Kayyal H,
922 Chandran SK, Khamaisy M, Sharma V, Rosenblum K (2019) Activity of Insula to
923 Basolateral Amygdala Projecting Neurons is Necessary and Sufficient for Taste Valence
924 Representation. *The Journal of Neuroscience*.
- 925 Kepecs A, Lisman J (2003) Information encoding and computation with spikes and bursts. In:
926 *Network: Computation in Neural Systems*.
- 927 Kim EJ, Juavinett AL, Kyubwa EM, Jacobs MW, Callaway EM (2015) Three Types of Cortical
928 Layer 5 Neurons That Differ in Brain-wide Connectivity and Function. *Neuron* 88:1253–
929 1267.
- 930 Koren T, Yifa R, Amer M, Krot M, Boshnak N, Ben-Shaan TL, Azulay-Debby H, Zalay I,
931 Avishai E, Hajjo H, Schiller M, Haykin H, Korin B, Farfara D, Hakim F, Kobiler O,
932 Rosenblum K, Rolls A (2021) Insular cortex neurons encode and retrieve specific immune
933 responses. *Cell* 184.
- 934 Krabbe S, Gründemann J, Lüthi A (2018) Amygdala Inhibitory Circuits Regulate Associative
935 Fear Conditioning. *Biological Psychiatry* 83:800–809.
- 936 Kuba H, Oichi Y, Ohmori H (2010) Presynaptic activity regulates Na⁺ channel distribution at the
937 axon initial segment. *Nature* 465.
- 938 Kuhlman SJ, Olivas ND, Tring E, Ikrar T, Xu X, Trachtenberg JT (2013) A disinhibitory
939 microcircuit initiates critical-period plasticity in the visual cortex. *Nature* 501:543–546
940 Available at:
941 <http://www.ncbi.nlm.nih.gov/pubmed/23975100>
942 <http://www.pubmedcentral.nih.gov/articlerender.fcgi?artid=PMC3962838>.
- 943 Lavi K, Jacobson GA, Rosenblum K, Lüthi A (2018) Encoding of Conditioned Taste Aversion in

- 944 Cortico-Amygdala Circuits. *Cell Reports* 24:278–283.
- 945 Levitan D, Liu C, Yang T, Shima Y, Lin JY, Wachutka J, Marrero Y, Ghoddousi RAM, Beltrame
946 E da V, Richter TA, Katz DB, Nelson SB (2020) Deletion of *stk11* and *fos* in mouse bla
947 projection neurons alters intrinsic excitability and impairs formation of long-term aversive
948 memory. *Elife* 9:1–29.
- 949 Lin JY, Amodeo LR, Arthurs J, Reilly S (2012) Taste neophobia and palatability: The pleasure of
950 drinking. *Physiology and Behavior* 106:515–519.
- 951 Livneh Y, Andermann ML (2021) Cellular activity in insular cortex across seconds to hours:
952 Sensations and predictions of bodily states. *Neuron*:S0896-6273(21)00653-X.
- 953 Livneh Y, Ramesh RN, Burgess CR, Levandowski KM, Madara JC, Fenselau H, Goldey GJ,
954 Diaz VE, Jikomes N, Resch JM, Lowell BB, Andermann ML (2017) Homeostatic circuits
955 selectively gate food cue responses in insular cortex. *Nature* 546:611–616 Available at:
956 <http://dx.doi.org/10.1038/nature22375>.
- 957 Livneh Y, Sugden AU, Madara JC, Essner RA, Flores VI, Sugden LA, Resch JM, Lowell BB,
958 Andermann ML (2020) Estimation of Current and Future Physiological States in Insular
959 Cortex. *Neuron* 105:1094-1111.e10.
- 960 Lovero KL, Simmons AN, Aron JL, Paulus MP (2009) Anterior insular cortex anticipates
961 impending stimulus significance. *Neuroimage* 45:976–983.
- 962 Luo YX, Galaj E, Ma YY (2021) Differential alterations of insular cortex excitability after
963 adolescent or adult chronic intermittent ethanol administration in male rats. *Journal of*
964 *Neuroscience Research* 99.
- 965 Maffei A, Haley M, Fontanini A (2012) Neural processing of gustatory information in insular
966 circuits. *Current Opinion in Neurobiology*.
- 967 Maglio LE, Noriega-Prieto JA, Maroto IB, Martin-Cortecero J, Muñoz-Callejas A, Callejo-
968 Móstoles M, de Sevilla DF (2021) Igf-1 facilitates extinction of conditioned fear. *Elife* 10.
- 969 Mickley GA, Kenmuir CL, McMullen CA, Snyder A, Yocom AM, Likins-Fowler D, Valentine
970 EL, Weber B, Biada JM (2004) Long-term age-dependent behavioral changes following a
971 single episode of fetal N-methyl-D-Aspartate (NMDA) receptor blockade. *BMC*
972 *Pharmacology* 4:1–16.
- 973 Mishra P, Narayanan R (2015) High-conductance states and A-type K⁺ channels are potential
974 regulators of the conductance-current balance triggered by HCN channels. *Journal of*
975 *Neurophysiology* 113.
- 976 Morrison DJ, Rashid AJ, Yiu AP, Yan C, Frankland PW, Josselyn SA (2016) Parvalbumin
977 interneurons constrain the size of the lateral amygdala engram. *Neurobiology of Learning*
978 *and Memory* 135:91–99 Available at: <http://dx.doi.org/10.1016/j.nlm.2016.07.007>.
- 979 Mumford D (1991) On the computational architecture of the neocortex - I. The role of the

- 980 thalamo-cortical loop. *Biological Cybernetics* 65:135–145.
- 981 Mumford D (1992) On the computational architecture of the neocortex - II The role of cortico-
982 cortical loops. *Biological Cybernetics* 66:241–251.
- 983 Nachman M, Ashe JH (1973) Learned taste aversions in rats as a function of dosage,
984 concentration, and route of administration of LiCl. *Physiology and Behavior* 10:73–78.
- 985 Nicolas C, Ju A, Wu W, Eldirdiri H, Delcasso S, Jacky D, Supiot L, Fomari C, Verite A, Masson
986 M, Rodriguez-Rozada S, Wiegert SJ, Beyeler A (2022) Linking emotional valence and
987 anxiety in a mouse insula-amygdala circuit. *Current Biology*.
- 988 Oh MM, Disterhoft JF (2020) Learning and aging affect neuronal excitability and learning.
989 *Neurobiology of Learning and Memory* 167.
- 990 Owen SF, Berke JD, Kreitzer AC (2018) Fast-Spiking Interneurons Supply Feedforward Control
991 of Bursting, Calcium, and Plasticity for Efficient Learning. *Cell* 172.
- 992 Piette CE, Baez-Santiago MA, Reid EE, Katz DB, Moran A (2012) Inactivation of basolateral
993 amygdala specifically eliminates palatability-related information in cortical sensory
994 responses. *Journal of Neuroscience* 32:9981–9991.
- 995 Preuschoff K, Quartz SR, Bossaerts P (2008) Human insula activation reflects risk prediction
996 errors as well as risk. *Journal of Neuroscience* 28:2745–2752.
- 997 Price AE, Stutz SJ, Hommel JD, Anastasio NC, Cunningham KA (2019) Anterior insula activity
998 regulates the associated behaviors of high fat food binge intake and cue reactivity in male
999 rats. *Appetite* 133:231–239.
- 1000 Ranck JB (1973) Studies on single neurons in dorsal hippocampal formation and septum in
1001 unrestrained rats. Part I. Behavioral correlates and firing repertoires. *Experimental*
1002 *Neurology* 41:462–531.
- 1003 Rieger NS, Varela JA, Ng AJ, Granata L, Djerdjaj A, Brenhouse HC, Christianson JP (2022)
1004 Insular cortex corticotropin-releasing factor integrates stress signaling with social affective
1005 behavior. *Neuropsychopharmacology*.
- 1006 Rodríguez-Durán LF, Martínez-Moreno A, Escobar ML, Rodríguez-Duran LF, Martínez-Moreno
1007 A, Escobar ML (2017) Bidirectional modulation of taste aversion extinction by insular
1008 cortex LTP and LTD. *Neurobiology of Learning and Memory* 142:85–90.
- 1009 Rogers-Carter MM, Djerdjaj A, Gribbons KB, Varela JA, Christianson JP (2019) Insular cortex
1010 projections to nucleus accumbens core mediate social approach to stressed juvenile rats.
1011 *Journal of Neuroscience* 39:8717–8729.
- 1012 Rogers-Carter MM, Varela JA, Gribbons KB, Pierce AF, McGoey MT, Ritchey M, Christianson
1013 JP (2018) Insular cortex mediates approach and avoidance responses to social affective
1014 stimuli. *Nature Neuroscience* 21:404–414 Available at: [http://dx.doi.org/10.1038/s41593-](http://dx.doi.org/10.1038/s41593-018-0071-y)
1015 [018-0071-y](http://dx.doi.org/10.1038/s41593-018-0071-y).

- 1016 Rolls BJ, Rolls ET, Rowe EA, Sweeney K (1981) Sensory specific satiety in man. *Physiology*
1017 *and Behavior* 27.
- 1018 Rosenblum K, Berman DE, Hazvi S, Lamprecht R, Dudai Y (1997) NMDA receptor and the
1019 tyrosine phosphorylation of its 2B subunit in taste learning in the rat insular cortex. *Journal*
1020 *of Neuroscience* 17:5129–5135.
- 1021 Russell JA (1980) A circumplex model of affect. *Journal of Personality and Social Psychology*
1022 39:1161–1178.
- 1023 Sadacca BF, Rothwax JT, Katz DB (2012) Sodium concentration coding gives way to evaluative
1024 coding in cortex and amygdala. *Journal of Neuroscience* 32.
- 1025 Samengo I, Mato G, Elijah DH, Schreiber S, Montemurro MA (2013) Linking dynamical and
1026 functional properties of intrinsically bursting neurons. *Journal of Computational*
1027 *Neuroscience* 35.
- 1028 Santini E, Quirk GJ, Porter JT (2008) Fear conditioning and extinction differentially modify the
1029 intrinsic excitability of infralimbic neurons. *Journal of Neuroscience* 28:4028–4036.
- 1030 Schachtman TR, Brown AM, Miller RR (1985) Reinstatement-induced recovery of a taste-LiCl
1031 association following extinction. *Animal Learning & Behavior* 13:223–227.
- 1032 Schier LA, Spector AC (2019) The functional and neurobiological properties of bad taste.
1033 *Physiological Reviews*.
- 1034 Sehgal M, Song C, Ehlers VL, Moyer JR (2013) Learning to learn - Intrinsic plasticity as a
1035 metaplasticity mechanism for memory formation. *Neurobiology of Learning and Memory*
1036 105:186–199.
- 1037 Senn V, Wolff SBE, Herry C, Grenier F, Ehrlich I, Gründemann J, Fadok JP, Müller C, Letzkus
1038 JJ, Lüthi A (2014) Long-range connectivity defines behavioral specificity of amygdala
1039 neurons. *Neuron* 81:428–437.
- 1040 Shah MM (2014) Cortical HCN channels: function, trafficking and plasticity. *The Journal of*
1041 *Physiology* 592:2711–2719.
- 1042 Shai AS, Anastassiou CA, Larkum ME, Koch C (2015) Physiology of Layer 5 Pyramidal
1043 Neurons in Mouse Primary Visual Cortex: Coincidence Detection through Bursting. *PLoS*
1044 *Computational Biology* 11.
- 1045 Shao LR, Halvorsrud R, Borg-Graham L, Storm JF (1999) The role of BK-type Ca²⁺-dependent
1046 K⁺ channels in spike broadening during repetitive firing in rat hippocampal pyramidal cells.
1047 *Journal of Physiology* 521:135–146.
- 1048 Sharma V, Ounallah-Saad H, Chakraborty D, Hleihil M, Sood R, Barrera I, Edry E, Kolatt
1049 Chandran S, ben Tabou de Leon S, Kaphzan H, Rosenblum K (2018) Local Inhibition of
1050 PERK Enhances Memory and Reverses Age-Related Deterioration of Cognitive and
1051 Neuronal Properties. *The Journal of Neuroscience*.

- 1052 Shor OL, Fidzinski P, Behr J (2009) Muscarinic acetylcholine receptors and voltage-gated
1053 calcium channels contribute to bidirectional synaptic plasticity at CA1-subiculum synapses.
1054 *Neuroscience Letters* 449.
- 1055 Siemian JN, Arenivar MA, Sarsfield S, Aponte Y (2021) Hypothalamic control of interoceptive
1056 hunger. *Current Biology* 31.
- 1057 Slouzkey I, Maroun M (2016) PI3-kinase cascade has a differential role in acquisition and
1058 extinction of conditioned fear memory in juvenile and adult rats. *Learning and Memory*
1059 23:723–731.
- 1060 Song C, Detert JA, Sehgal M, Moyer JR (2012) Trace fear conditioning enhances synaptic and
1061 intrinsic plasticity in rat hippocampus. *Journal of Neurophysiology* 107:3397–3408.
- 1062 Song C, Ehlers VL, Moyer JR (2015) Trace fear conditioning differentially modulates intrinsic
1063 excitability of medial prefrontal cortex–basolateral complex of amygdala projection neurons
1064 in infralimbic and prelimbic cortices. *Journal of Neuroscience* 35:13511–13524.
- 1065 Song C, Moyer JR (2018) Layer- and subregion-specific differences in the neurophysiological
1066 properties of rat medial prefrontal cortex pyramidal neurons. *Journal of Neurophysiology*.
- 1067 Soto A, Gasalla P, Begega A, López M (2017) c-Fos activity in the insular cortex, nucleus
1068 accumbens and basolateral amygdala following the intraperitoneal injection of saccharin
1069 and lithium chloride. *Neuroscience Letters*.
- 1070 Staff NP, Jung HY, Thiagarajan T, Yao M, Spruston N (2000) Resting and active properties of
1071 pyramidal neurons in subiculum and CA1 of rat hippocampus. *Journal of Neurophysiology*.
- 1072 Stone ME, Fontanini A, Maffei A (2020) Synaptic integration of thalamic and limbic inputs in
1073 rodent gustatory cortex. *eNeuro*.
- 1074 Suzuki A, Josselyn SA, Frankland PW, Masushige S, Silva AJ, Kida S (2004) Memory
1075 reconsolidation and extinction have distinct temporal and biochemical signatures. *Journal of*
1076 *Neuroscience* 24:4787–4795.
- 1077 Turrigiano G (2011) Too many cooks? Intrinsic and synaptic homeostatic mechanisms in cortical
1078 circuit refinement. *Annual Review of Neuroscience* 34.
- 1079 Ventura R, Morrone C, Puglisi-Allegra S (2007) Prefrontal/accumbal catecholamine system
1080 determines motivational salience attribution to both reward-and aversion-related stimuli.
1081 *Proc Natl Acad Sci U S A* 104:5181–5186.
- 1082 Vincis R, Chen K, Czarnecki L, Chen J, Fontanini A (2020) Dynamic Representation of Taste-
1083 Related Decisions in the Gustatory Insular Cortex of Mice. *Current Biology*.
- 1084 Vincis R, Fontanini A (2016) A gustocentric perspective to understanding primary sensory
1085 cortices. *Current Opinion in Neurobiology* 40:118–124 Available at:
1086 <http://dx.doi.org/10.1016/j.conb.2016.06.008>.
- 1087 Wang L, Gillis-Smith S, Peng Y, Zhang J, Chen X, Salzman CD, Ryba NJP, Zuker CS (2018)

- 1088 The coding of valence and identity in the mammalian taste system. *Nature* 558:127–131
1089 Available at: <http://dx.doi.org/10.1038/s41586-018-0165-4>.
- 1090 Wozny C, Maier N, Schmitz D, Behr J (2008) Two different forms of long-term potentiation at
1091 CA1-subiculum synapses. *Journal of Physiology* 586.
- 1092 Wu C-H, Ramos R, Katz DB, Turrigiano GG (2021) Homeostatic synaptic scaling establishes the
1093 specificity of an associative memory. *Current Biology*.
- 1094 Wu Y, Chen C, Chen M, Qian K, Lv X, Wang H, Jian L, Yu L, Zhu M, Qiu S (2020) The anterior
1095 insular cortex unilaterally controls feeding in response to aversive visceral stimuli in mice.
1096 *Nat Commun* 11.
- 1097 Xia F, Richards BA, Tran MM, Josselyn SA, Takehara-Nishiuchi K, Frankland PW, Bartos M,
1098 Xia F, Richards BA, Tran MM, Josselyn SA, Takehara-Nishiuchi K, Frankland PW (2017)
1099 Parvalbumin-positive interneurons mediate neocortical-hippocampal interactions that are
1100 necessary for memory consolidation. *Elife* 6:1–25 Available at:
1101 <https://doi.org/10.7554/eLife.27868.001>.
- 1102 Yang SS, Li YC, Coley AA, Chamberlin LA, Yu P, Gao WJ (2018) Cell-type specific
1103 development of the hyperpolarization-activated current, I_h , in prefrontal cortical neurons.
1104 *Frontiers in Synaptic Neuroscience* 10.
- 1105 Yazaki-Sugiyama Y, Kang S, Cteau H, Fukai T, Hensch TK (2009) Bidirectional plasticity in
1106 fast-spiking GABA circuits by visual experience. *Nature*.
- 1107 Yeomans MR (1998) Taste, palatability and the control of appetite. *Proceedings of the Nutrition*
1108 *Society* 57.
- 1109 Yiannakas A, Kolatt Chandran S, Kayyal H, Gould N, Khamaisy M, Rosenblum K (2021)
1110 Parvalbumin interneuron inhibition onto anterior insula neurons projecting to the basolateral
1111 amygdala drives aversive taste memory retrieval. *Current Biology* 31:1–15.
- 1112 Yousuf H, Ehlers VL, Sehgal M, Song C, Moyer JR (2019) Modulation of intrinsic excitability
1113 as a function of learning within the fear conditioning circuit. *Neurobiology of Learning and*
1114 *Memory* 167.
- 1115 Zeldenrust F, Wadman WJ, Englitz B (2018) Neural coding with bursts—Current state and future
1116 perspectives.
- 1117 Zhao Z, Soria-Gómez E, Varilh M, Covelo A, Julio-Kalajzić F, Cannich A, Castiglione A,
1118 Vanhoutte L, Duveau A, Zizzari P, Beyeler A, Cota D, Bellocchio L, Busquets-Garcia A,
1119 Marsicano G (2020) A Novel Cortical Mechanism for Top-Down Control of Water Intake.
1120 *Current Biology* 30.
- 1121

1122 Figure legends

1123 Figure 1: Retrieval of appetitive and novel taste increases excitability in LIV-VI aIC-
1124 BLA projection neurons

1125 A) Diagrammatic representation of experimental procedures. Following surgery and stereotaxic
1126 delivery of ssAAV_retro2-hSyn1-chi-mCherry-WPRE-SV40p(A) into the BLA, mice were
1127 allowed 4 weeks of recovery. Animals were subsequently assigned to treatment groups and
1128 trained to drink from pipettes (see Methods). We compared the intrinsic properties of LIV-VI
1129 aIC-BLA neurons among the Water (n=6 animals, 23 cells), Saccharin 1x (n=5 animals, 20 cells),
1130 Saccharin 1x(4h) (n=4 animals, 17 cells), Saccharin 5x (n=6 animals, 18 cells) and Quinine 1x
1131 groups (n=4 animals, 19 cells), as well as a Cage control group (n=4 animals, 19 cells) that
1132 underwent surgery and stereotaxic delivery of ssAAV_retro2-hSyn1-chi-mCherry-WPRE-
1133 SV40p(A) at the BLA without water restriction.

1134 B) Graph showing the water consumption prior to treatment (mean \pm SD). There was no
1135 significant difference between water intakes between the groups before the treatment. One-Way
1136 ANOVA, $p= 0.9766$.

1137 C) Representative traces of LIV-VI aIC-BLA projecting neurons from the six treatment groups.
1138 Scale bars 20 mV vertical and 50ms horizontal from 300 pA step.

1139 D) The dependence of firing rate on current step magnitude in LIV-VI aIC-BLA neurons was
1140 significantly different among the treatment groups. Excitability in the Saccharin 1x was
1141 increased compared to all other groups. Two-way repeated measures ANOVA, Current x
1142 Treatment: $p<0.0001$; Cage control vs. Saccharin 1x: $**p<0.01$, $***p<0.001$; Saccharin 1x vs.
1143 Saccharin 1x (4hr) : $\#p<0.05$, $##p<0.01$, $####p<0.0001$; Water vs. Saccharin 1x: $\wedge p<0.05$,

1144 $\wedge p < 0.01$, $\wedge\wedge p < 0.001$; Saccharin 1x vs. Quinine 1x: $\$ p < 0.05$, $\$\$ p < 0.01$; Saccharin 1x vs.
1145 Saccharin 5x: $- p < 0.05$; Saccharin 1x (4hr) vs. Saccharin 5x : $+ p < 0.05$.

1146 E) Representative of all fAHP measurements in response to 500 msec step current injections.
1147 Scale bars 20 mV vertical and 50 msec horizontal.

1148 F) Representative of all action potential properties were taken. Scale bars 20 mV vertical and 5
1149 msec horizontal.

1150 G) Measurements for all input resistance, sag ratio and membrane time constants were analyzed
1151 in response to 1 sec, -150pA step current injection. P- peak voltage, S- steady state voltage. Scale
1152 bars 5 mV vertical and 100 msec horizontal.

1153 H) Significant differences were observed among the treatment groups in terms of fAHP. Cage
1154 control (9.191 ± 1.449 mV), Water (8.150 ± 0.8288 mV), Saccharin 1x (3.016 ± 0.9423 mV),
1155 Quinine 1x (13.58 ± 1.562 mV) Saccharin 5x (8.158 ± 1.356 mV), Saccharin 1x (4hrs) ($5.989 \pm$
1156 1.074 mV), One-Way ANOVA, $p < 0.0001$.

1157 I) Action potential half-width in the Saccharin 1x group (0.6005 ± 0.03260 msec) was
1158 significantly decreased compared to Saccharin 1x (4hr) 90.7765 ± 0.03641 msec), One-Way
1159 ANOVA, $p = 0.0065$.

1160 J) The membrane time constant was significantly different between the Saccharin 1x ($14.82 \pm$
1161 1.485 msec) and Saccharin 1x (4hrs) (26.21 ± 2.421 msec) groups and Cage control ($15.03 \pm$
1162 1.376 msec), One-Way ANOVA, $p = 0.0005$.

1163 For panels 1D, H, I and J: $*p < 0.05$, $**p < 0.01$, $***p < 0.001$, $****p < 0.0001$.

1164 All data are shown as mean \pm SEM.

1165

1166 Figure 2: Learned aversive taste memory retrieval suppresses the excitability of LIV-VI
1167 aIC-BLA projecting neurons

1168 A) Experimental design of behavioral procedures conducted to compare the intrinsic properties
1169 of LIV-VI aIC-BLA neurons following learned aversive taste memory retrieval (CTA retrieval -
1170 n=8 animals, 27 cells), appetitive retrieval for the same tastant (Saccharin 2x - n=5 animals, 20
1171 cells).

1172 B) Mice showed a significantly reduced saccharin consumption following learned aversive
1173 memory retrieval (N=8) compared to appetitive retrieval mice (n=5) group. $p=0.0085$, Mann
1174 Whitney test.

1175 C) Representative traces of LIV-VI aIC-BLA projecting neurons from the two treatment groups.
1176 Scale bars 20 mV vertical and 50ms horizontal from 300 pA step.

1177 D) The excitability of LIV-VI aIC-BLA in the Saccharin 2x group was significantly enhanced
1178 compared to CTA retrieval. Two-way repeated measures ANOVA, Current x Treatment:
1179 $p<0.0001$.

1180 E) Representative traces showing action potential measurements for both groups. Scale bar 20
1181 mV vertical and 2ms horizontal.

1182 F) Representative traces showing the input resistance and sag ratio measurements. Scale bar 10
1183 mV vertical and 100ms horizontal.

1184 G) Action potential amplitude in the CTA retrieval (56.21 ± 0.9978 mV) group was increased
1185 compared to Saccharin 2x (49.14 ± 1.568 mV), $p=0.0005$, Mann Whitney test.

1186 H) Input resistance in the CTA retrieval group ($136.4 \pm 9.064 \text{ M}\Omega$) was significantly decreased
1187 compared to Saccharin 2x ($181.1 \pm 11.7 \text{ M}\Omega$). $p=0.0036$, Unpaired t test.

1188 I) SAG ratio following CTA retrieval (13.41 ± 1.31) was significantly enhanced compared to
1189 Saccharin 2x (7.815 ± 1.176). $p=0.0037$, Unpaired t test.

1190 Data are shown as mean \pm SEM. * $p<0.05$, ** $p<0.01$, *** $p<0.001$, **** $p<0.0001$.

1191

1192 Figure 3: Extinction of CTA enhances, whereas reinstatement suppresses the excitability
1193 of LIV-VI aIC-BLA projecting neurons

1194 A) Experimental design of behavioral procedures conducted to compare the intrinsic properties
1195 of LIV-VI aIC-BLA neurons following CTA Extinction (n=5, animals, 14 cells) and
1196 Reinstatement (n=3 animals, 15 cells).

1197 B) The graph showing the reduced aversion following the successful extinction in both treatment
1198 groups.

1199 C) Data showing the saccharin consumption on the test day following successful extinction and
1200 Reinstatement of CTA. CTA reinstated mice showed significantly reduced saccharin
1201 consumption compared to extinguished mice. $p=0.0179$, Mann Whitney test.

1202 D) Representative traces of LIV-VI aIC-BLA projection neurons firing from the two treatment
1203 groups. Scale bars 20 mV and 50ms horizontal from 300 pA step.

1204 E) Excitability in LIV-VI aIC-BLA neurons was significantly different among the treatment
1205 groups. Two-Way repeated measures ANOVA, Current x Treatment: $p<0.0001$.

1206 F) Action potential threshold in the Reinstatement group ($-29.43 \pm 1.731 \text{ mV}$) was enhanced

1207 compared to Extinction (-36.06 ± 1.481 mV). $p=0.0076$, Unpaired t test.

1208 G) The membrane time constant following Reinstatement (25.48 ± 1.58 msec) was significantly
1209 enhanced compared to Extinction (17.55 ± 2.684 msec, $p=0.047$). $p=0.0153$, Unpaired t test.

1210 For panels 5D-F: * $p<0.05$, ** $p<0.01$, *** $p<0.001$, **** $p<0.0001$.

1211 All data are shown as mean \pm SEM.

1212

1213 Figure 4: Innately aversive taste is correlated with high fAHP, and prolonged conflicting
1214 experiences is correlated with an increased AP half-width in LIV-VI aIC-BLA projecting
1215 neurons

1216 We compared the intrinsic properties of LIV-VI aIC-BLA neurons among the Saccharin 1x (n=5
1217 animals, 20 cells), Quinine 1x (n=4 animals, 19 cells), Saccharin 2x (n=5 animals, 20 cells), CTA
1218 retrieval (n=8, 27 cells), Extinction (n=5 animals, 14 cells) and Reinstatement (n=3 animals, 15
1219 cells) groups.

1220 A) Groups associated with positive taste valence (Saccharin 1x, Saccharin 2x, Extinction),
1221 exhibited significantly increased excitability compared to innate or learned negative taste valence
1222 groups (Quinine 1x, CTA retrieval and Reinstatement). Two-way repeated measures ANOVA,
1223 Current x Treatment: $p<0.0001$; Saccharin 2x vs. CTA retrieval: * p ; Saccharin 2x vs.
1224 Reinstatement: # p ; Saccharin 2x vs Quinine 1x: $p\$$; Saccharin 1x vs. CTA retrieval: p^{\wedge} ;
1225 Saccharin 1x vs. Quinine 1x: $p\%$; Saccharin 1x vs reinstatement: $p+$; Extinction vs. CTA
1226 retrieval: $p@$; Extinction vs. Reinstatement: $p\&$; Extinction vs. Quinine 1x: $p-$.

1227 B) fAHP was significantly enhanced in response to Quinine 1x (13.56 ± 1.562 mV) compared to

1228 all other groups. Significant differences were also observed between Saccharin 1x ($3.016 \pm$
1229 0.9423 mV), Saccharin 2x (5.223 ± 0.8217 mV), and CTA retrieval (7.97 ± 1.018 mV,
1230 $p=0.0036$). Extinction (4.731 ± 1.021 mV) and Reinstatement (5.932 ± 1.292 mV). One-Way
1231 ANOVA, $p<0.0001$.

1232 C) Input resistance was significantly different between Saccharin 2x (181.1 ± 11.7 M Ω) and CTA
1233 retrieval (136.4 ± 9.064 M Ω), $p= 0.0352$. Conversely, Input resistance in Saccharin 1X ($145.8 \pm$
1234 12.56), Quinine 1X (146 ± 9.094), Extinction (151.1 ± 15.63), and Reinstatement groups was
1235 similar. One-Way ANOVA, $p= 0.0213$.

1236 D) SAG ratio was significantly different between Saccharin 2x (7.815 ± 1.176) and CTA retrieval
1237 (13.41 ± 1.31), $p= 0.0209$. Conversely, SAG ratio in Saccharin 1x (10.89 ± 1.621), Quinine 1x
1238 (12.13 ± 1.23), Extinction (12.37 ± 1.471) and Reinstatement (9.245 ± 0.884) groups was similar
1239 One-Way ANOVA, $p= 0.0286$.

1240 E) Action potential amplitude in the Quinine 1x group (57.11 ± 1.376 mV), and CTA retrieval
1241 (56.21 ± 0.9978 mV), was significantly increased compared to Saccharin 2x (49.14 ± 1.568 mV,
1242 $p= 0.0175$, and 0.0229 , respectively). Conversely, action potential attitude in the Saccharin 1x
1243 (52.03 ± 1.308 mV), Extinction (55.09 ± 2.122 mV) and Reinstatement (53.1 ± 2.906 mV)
1244 groups was similar. One-Way ANOVA, $p = 0.0061$.

1245 F) Action potential half-width following Extinction (0.7386 ± 0.03145 msec) and Reinstatement
1246 (0.8187 ± 0.06929 msec) was elevated compared to Saccharin 1x (0.6005 ± 0.03260 msec),
1247 Saccharin 2x (0.5780 ± 0.02994 msec) as well as CTA retrieval (0.5959 ± 0.02080 msec, but no
1248 with Quinine 1x (0.6300 ± 0.03555 msec). One-Way ANOVA, $p = 0.0002$.

1249 G) The membrane time constant in the Saccharin 1x (14.82 ± 1.485 msec) group was

1250 significantly suppressed compared to Reinstatement (25.48 ± 1.58 msec, $p= 0.0043$) groups was.
1251 Differences between CTA retrieval (20.96 ± 1.724 msec, $p=0.0189$), Quinine 1x (21.55 ± 1.638
1252 msec), Saccharin 2x (19.28 ± 1.837 msec) and Extinction (17.55 ± 2.684 msec) groups failed to
1253 reach significance. One-Way ANOVA, $p = 0.0047$.

1254

1255 Figure 5: The intrinsic properties of burst-spiking LIV-VI aIC-BLA projecting neurons
1256 represent taste experience and the probability for further learning

1257 A) Data across all intrinsic properties from BS LIV-VI aIC-BLA neurons of the Saccharin 1x,
1258 Saccharin 2x and Extinction groups were combined and assigned to the Low predictive
1259 following memory group (32 BS cells). Conversely, the intrinsic properties of BS LIV-VI aIC-
1260 BLA neurons from animals having undergone CTA retrieval, 5x Saccharin, and Reinstatement
1261 were combined and assigned to the High predictive following memory group (31 BS cells). The
1262 resultant three-dimensional scatter representation of the two groups encompassed Excitability at
1263 350pA; AP amplitude, AP halfwidth, AP threshold; fAHP, mAHP, sAHP; IR, Rheobase, RMP,
1264 SAG ratio and τ in BS LIV-VI aIC-BLA neurons.

1265 B) Three-dimensional representation of the contribution of individual parameters (loadings
1266 matrix) to the principal components segregating the two groups of treatments (scores matrix).

1267

1268 Figure 6: A model for excitability changes in IV-VI aIC-BLA neurons when the taste
1269 salience is low and highly predictive following the taste memory

1270 • The unpredictability of future valence outcomes: Novel appetitive taste experiences
1271 /extinction of previously learned aversive taste experiences, increases the excitability

1272 (blue arrow) of aIC-BLA projecting neurons (red). This increased excitability is specific
1273 to the deep-layer aIC-BLA projecting neurons (LIV-VI).

1274 • When the taste valence is highly predictable (familiar/aversive), excitability is reduced in
1275 LIV-VI aIC-BLA projecting neurons (red arrow).

1276 • LIV-VI aIC-BLA neurons remain excitable facilitating the association of the taste
1277 memory trace with visceral pain when the stimulus is not adequately predictive of the
1278 outcome of the sensory experience.

1279

1280 Extended figures and Tables

1281

1282 Extended Figure 1-1: Histological verification of rAAV-mCherry virus expression and
1283 locations of whole- cell patch clamp recordings

1284 A) A representative image showing the distribution of retrograde injections into the BLA and
1285 aIC-BLA projection neuron at aIC.

1286 B) Mean localization of BLA projecting neurons of the agranular aIC used for
1287 electrophysiological whole cell recordings.

1288 Extended Figure 1-2: The ratio of burst-spiking and regular spiking LIV-VI aIC-BLA
1289 projecting neurons changes in relation to the uncertainty associated with taste experiences

1290 A) Representative traces from Burst (BS) and Regular (RS) spiking LIV-VI aIC-BLA projecting
1291 neurons in response to rheobase current injections. The neurons showing doublets or triplets in

1292 response to rheobase current injection were considered BS. The neurons showing single spike in
1293 response to rheobase current injection considered RS. Scale bars 20 mV and 100 msec.

1294 B) Pie charts showing the change in the ratio of BS vs RS LIV-VI aIC-BLA projection neurons,
1295 expressed as a percentage of the sampled population across the Saccharin 1x, Saccharin 2x,
1296 Saccharin 5x, CTA retrieval, Extinction, and Reinstatement groups.

1297 C) Heat map summary of the change in the ratio of BS vs RS LIV-VI aIC-BLA projection
1298 neurons, expressed as a percentage of the sampled population across the six treatment groups.

1299

1300 Extended Figure 1-3: Appetitive novel taste alters the intrinsic properties of burst spiking
1301 LIV-VI aIC-BLA neurons

1302 We compared the intrinsic properties of BS and RS LIV-VI aIC-BLA neurons among the Cage
1303 control (n=13 cells), Water (n= 11cells), Saccharin 1X (n=17 cells), Quinine 1x (n=9 cells),
1304 Saccharin 5x (n=10 cells) and Saccharin 1x (4hrs, n=6 cells).

1305 A) Excitability in BS LIV-VI aIC-BLA was not significantly different among the treatment
1306 groups. Two-Way repeated measures ANOVA, Current x Treatment: $p < 0.0001$, Group interaction
1307 $p = 0.0666$.

1308 B) fAHP was significantly enhanced in Quinine 1x (13.67 ± 2.681 mV) and Saccharin 5x (11.30
1309 ± 1.727 mV) BS neurons compared to Saccharin 1x BS neurons (2.870 ± 1.044 mV). One-Way
1310 ANOVA, $P = 0.0004$.

1311 C) Action potential amplitude was significantly different between the groups. Cage controls
1312 (56.27 ± 1.147 mV), Water (54.21 ± 1.572 mV), Saccharin 1x (51.64 ± 1.473 mV), Quinine 1X
1313 (58.86 ± 2.003 mV), Saccharin 5x (58.40 ± 1.812 mV), and Saccharin 1x (4hr) (46.79 ± 4.359

1314 mV). One-Way ANOVA, P= 0.0097.

1315 D) Action potential half-width in BS LIV-VI aIC-BLA neurons of the Saccharin 1x (4 hrs.)
1316 group ($0.8850 \pm 0.05943\text{ms}$) was increased compared to the Saccharin 1x (1hr) group - $0.5976 \pm$
1317 0.03555ms . One-Way ANOVA, P=0.0139.

1318 E) Action potential threshold was not significantly different between the groups. Cage control (-
1319 31.83 ± 2.971 mV), Water (-29.27 ± 2.060 mV), Saccharin 1x (-30.73 ± 2.385 mV), Quinine 1x (-
1320 29.35 ± 3.071 mV), Saccharin 5x (-30.38 ± 2.493 mV), and Saccharin 1x (4hr) (-34.61 ± 2.174
1321 mV). One-Way ANOVA, P= 0.7652.

1322 F) Input resistance was similar among the different treatment groups. Cage control ($118.4 \pm$
1323 9.771 M Ω), Water (136.5 ± 14.40 M Ω), Saccharin 1x (146.6 ± 14.22 M Ω), Quinine 1x ($139.2 \pm$
1324 16.86 M Ω), Saccharin 5x (156.1 ± 22.85 M Ω), and Saccharin 1x (4hr) (154.9 ± 22.41 M Ω).
1325 One-Way ANOVA, P= 0.6304.

1326 G) SAG ratio was not significantly different between the groups. Cage control (14.91 ± 2.195),
1327 Water (8.751 ± 2.021), Saccharin 1x (11.67 ± 1.790), Quinine 1x (14.15 ± 2.159), Saccharin 5x
1328 (11.92 ± 3.395), and Saccharin 1x (4hr) (14.99 ± 2.770). One-Way ANOVA, P= 0.2232.

1329 H) Membrane time constant was significantly different among the treatment groups. Cage
1330 control (14.71 ± 1.944 msec), Water (18.03 ± 2.309 msec), Saccharin 1x (14.27 ± 1.666 msec),
1331 Quinine 1x (23.21 ± 2.717 msec), Saccharin 5x (17.11 ± 2.296 msec), and Saccharin 1x (4hr)
1332 (26.09 ± 5.331 msec). One-Way ANOVA, P= 0.0321.

1333 Data are shown as mean \pm SEM. *p<0.05, **p<0.01.

1334

1335

1336

1337 Extended Figure 2-1: Learned aversive taste memory retrieval suppresses the excitability
1338 of burst spiking LIV-VI aIC-BLA neurons

1339

1340 We compared the intrinsic properties of BS and RS LIV-VI aIC-BLA neurons following
1341 Saccharin 2xs (BS=13, RS=7, cells) and CTA memory retrieval (BS=12, RS=15, cells).

1342 A) Excitability in BS LIV-VI aIC-BLA neurons was significantly reduced in the CTA retrieval
1343 group compared to Saccharin 2x. Two-Way repeated measures ANOVA, Current x Treatment:
1344 $p < 0.0001$.

1345 B) Input resistance in BS LIV-VI aIC-BLA neurons was significantly enhanced in the Saccharin
1346 2x ($180.3 \pm 15.15 \text{ M}\Omega$) compared to CTA retrieval ($110.9 \pm 12.98 \text{ M}\Omega$). Unpaired t test, $p =$
1347 0.0022 .

1348 C) Action potential amplitude in BS LIV-VI aIC-BLA neurons was significantly increased in the
1349 CTA retrieval group compared to Saccharin 2x ($46.18 \pm 1.666 \text{ mV}$), and CTA retrieval ($57.87 \pm$
1350 1.678 mV). Mann Whitney test, $p < 0.0001$.

1351 D) SAG ratio in BS LIV-VI aIC-BLA neurons was significantly suppressed in the Saccharin 2x
1352 (7.017 ± 1.317) compared to CTA retrieval (16.8 ± 1.869). Mann Whitney test, $p = 0.0005$.

1353 E) Representative traces of RS LIV-VI aIC-BLA neurons firing from the two treatments. Scale
1354 bars 20 mV vertical and 50ms horizontal in response to 150 pA step current.

1355 F) Excitability in RS LIV-VI aIC-BLA neurons was similar in the CTA retrieval and Saccharin

1356 2x. Two-Way repeated measures ANOVA, Current x Treatment: $p= 0.0953$.

1357 G) Input resistance in RS LIV-VI aIC-BLA neurons was not significantly different in between
1358 the groups. Saccharin 2x ($182.6 \pm 19.62 \text{ M}\Omega$), and CTA retrieval ($156.7 \pm 10.11 \text{ M}\Omega$). Mann
1359 Whitney test, $p > 0.9999$.

1360 H) SAG ratio in RS LIV-VI aIC-BLA neurons was not significantly different between the
1361 groups. Saccharin 2x (9.297 ± 2.347), and CTA retrieval (10.71 ± 1.536). Mann Whitney test, $p=$
1362 0.5815 .

1363 I) Action potential amplitude in RS LIV-VI aIC-BLA neurons was not significantly different
1364 between the groups. Saccharin 2x ($54.62 \pm 2.058 \text{ mV}$), and CTA retrieval ($54.89 \pm 1.13 \text{ mV}$).
1365 Mann Whitney test, $p > 0.9999$.

1366 J) AP half-width in RS LIV-VI aIC-BLA neurons was significantly reduced following CTA
1367 memory retrieval ($0.5633 \pm 0.01703 \text{ msec}$) compared to the Saccharin 2x ($0.6614 \pm$
1368 0.04149 msec). Mann Whitney test, $p= 0.0200$.

1369 K) Membrane time constant was similar in both treatment groups. Saccharin 2x RS ($18.36 \pm$
1370 2.842 ms), and CTA memory retrieval RS ($24.08 \pm 2.023 \text{ msec}$). Mann Whitney test, $p= 0.0777$.

1371 Data are shown as mean \pm SEM. * $p < 0.05$, ** $p < 0.01$, *** $p < 0.001$, **** $p < 0.0001$.

1372

1373 Extended Figure 3-1: Extinction of CTA enhances excitability of burst spiking LIV-VI
1374 aIC-BLA projecting neurons

1375

1376 We compared the intrinsic properties of BS and RS LIV-VI aIC-BLA neurons following the

1377 Extinction (BS=11, RS=3, cells) and Reinstatement (BS=10, RS=5, cells).

1378 A) Excitability in BS LIV-VI aIC-BLA was significantly enhanced in Extinction group
1379 comparing to Reinstatement. Two-Way repeated measures ANOVA, Current x Treatment:
1380 $p < 0.0001$.

1381 B) sAHP in BS LIV-VI aIC-BLA neurons was significantly enhanced in the Extinction group (-
1382 2.104 ± 0.4466 mV) compared to Reinstatement (-3.804 ± 1.339 mV) neurons. Mann Whitney
1383 test, $p = 0.0230$.

1384 C) Action potential threshold in BS LIV-VI aIC-BLA neurons was significantly reduced in the
1385 Extinction group (-37.41 ± 1.636 mV) compared to Reinstatement (-27.5 ± 2.195 mV). Unpaired
1386 t test, $p = 0.0016$.

1387 D) Input resistance in BS LIV-VI aIC-BLA neurons was similar in the two treatment groups.
1388 Extinction (131.1 ± 13.93 M Ω) and Reinstatement BS (157.4 ± 10.56 M Ω). Mann Whitney test,
1389 $p = 0.1321$.

1390 E) SAG ratio in BS LIV-VI aIC-BLA neurons was enhanced following Extinction ($13.69 \pm$
1391 1.541) neurons compared to Reinstatement BS (9.124 ± 1.03). Unpaired t test, $p = 0.0262$.

1392 F) Membrane time constant in BS LIV-VI aIC-BLA neurons was significantly reduced in the
1393 Extinction group (14.52 ± 2.714 msec) compared to Reinstatement (26.93 ± 1.893) neurons.
1394 Mann Whitney test, $p = 0.0062$.

1395 G) Representative traces of RS LIV-VI aIC-BLA firing from two treatment groups. Scale bars 20
1396 mV vertical and 50 msec horizontal in response to 150 pA current step.

1397 H) Excitability of RS LIV-VI aIC-BLA neurons in both treatment groups.

1398 I) Input resistance in RS LIV-VI aIC-BLA neurons was similar in the Extinction (224.2 ± 21.29
1399 $M\Omega$) and Reinstatement ($221.2 \pm 18.9 M\Omega$) groups.

1400 J) SAG ratio in RS LIV-VI aIC-BLA neurons was not different between the Extinction ($7.515 \pm$
1401 2.666) and Reinstatement (9.486 ± 1.846) groups.

1402 K) Membrane time constant in RS LIV-VI aIC-BLA neurons was not different between the
1403 Extinction ($28.69 \pm 2.138\text{msec}$) and Reinstatement groups ($22.58 \pm 2.632\text{msec}$).

1404

1405 Extended Figure 5-1: PCA showing Burst vs Regular spiking LIV-VI aIC-BLA neurons
1406 all range of excitability vs 350 pA only

1407 A) PCA of BS and RS LIV-VI aIC-BLA neurons all range of excitability (50-350 pA and all
1408 other intrinsic properties measured). Sampled population across six treatment groups (Saccharin
1409 1x, Saccharin 2x, Saccharin 5x, CTA retrieval, Extinction, Reinstatement).

1410 B) PCA of BS and RS LIV-VI aIC-BLA neurons excitability of 350 pA only and all other
1411 intrinsic properties measured. Sampled population across six treatment groups (Saccharin 1x,
1412 Saccharin 2x, Saccharin 5x, CTA retrieval, Extinction, Reinstatement).

1413

1414 Extended Figure 5-2: PCA variable contributions and component loadings of BS and RS
1415 LIV-VI aIC-BLA projecting neurons

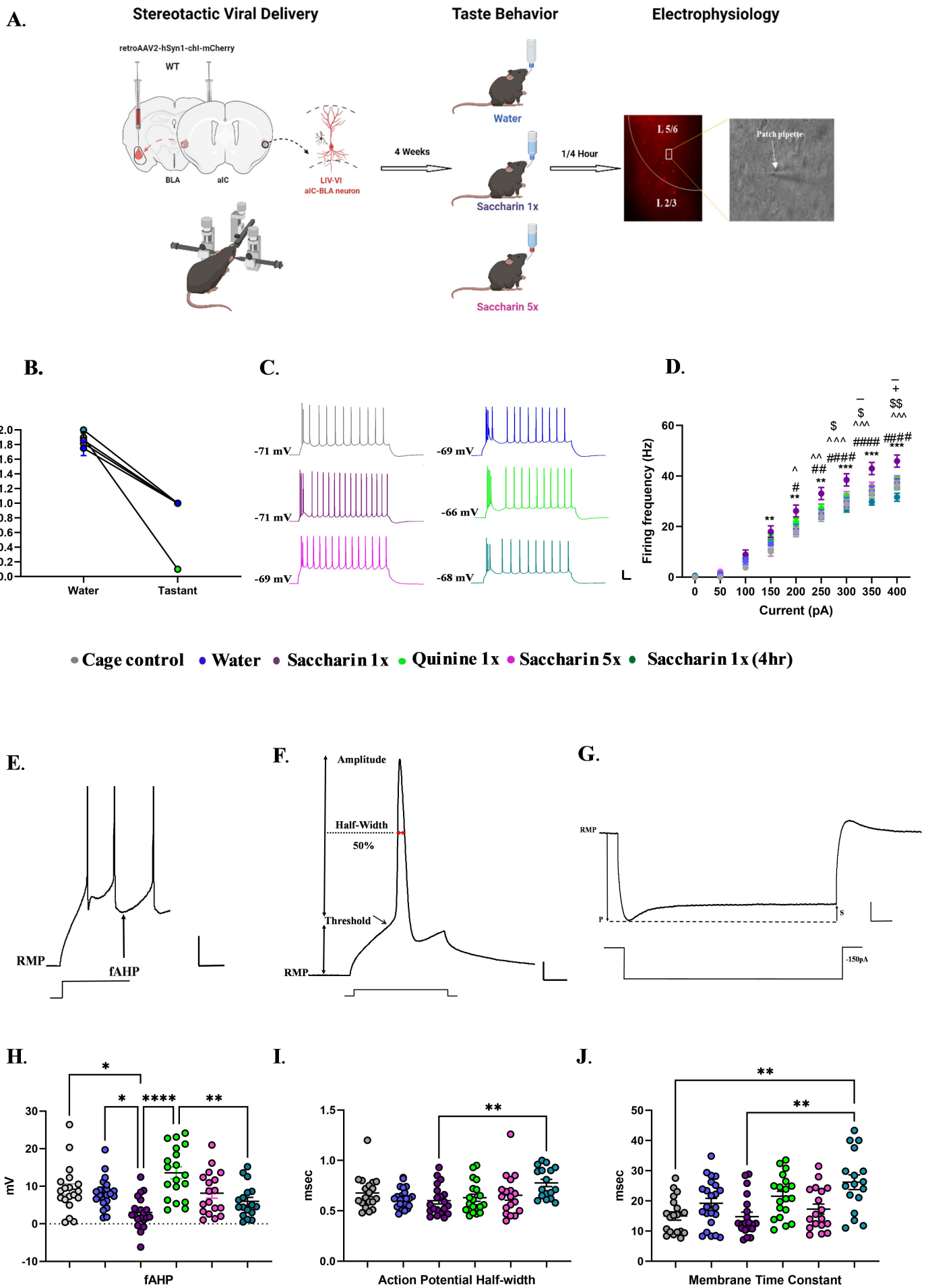
1416 A) Column chart demonstrating the individual and cumulative proportion of the variance
1417 accounted by principal components following PCA of BS LIV-VI aIC-BLA projecting neurons
1418 in the two groups of treatments (Saccharin 1x, Saccharin 2x, Extinction vs. CTA retrieval, 5x

1419 Saccharin, Reinstatement).

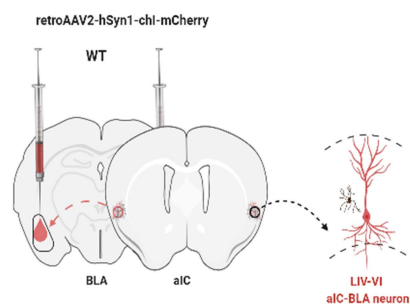
1420 B) Table summarizing the contribution of individual variables (loadings) to the coordinate value
1421 of the principal components segregating the two groups (score).

1422 C) Communalities table, demonstrating the amount of variance in each variable that is accounted
1423 for by the extraction of principal components. Initial communalities are estimates of the variance
1424 in each variable accounted for by all components or factors (=1.00).

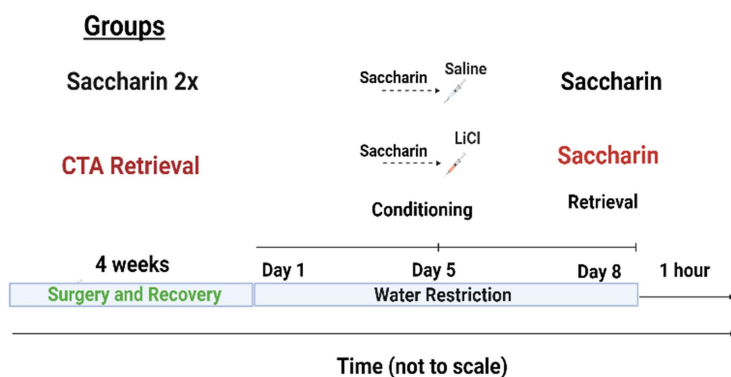
1425



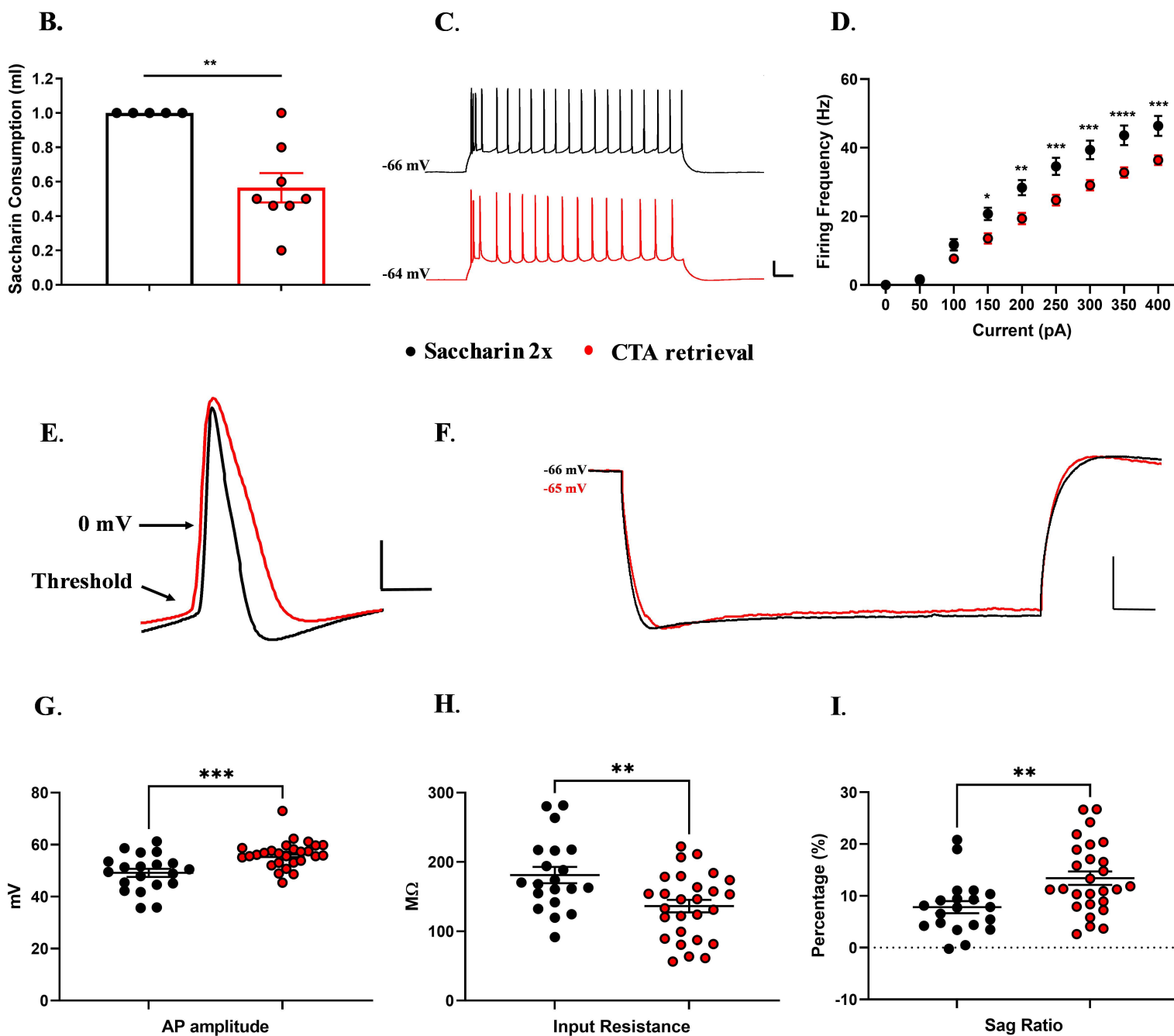
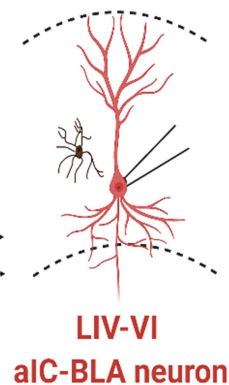
Stereotactic Viral Delivery



Taste Behavior

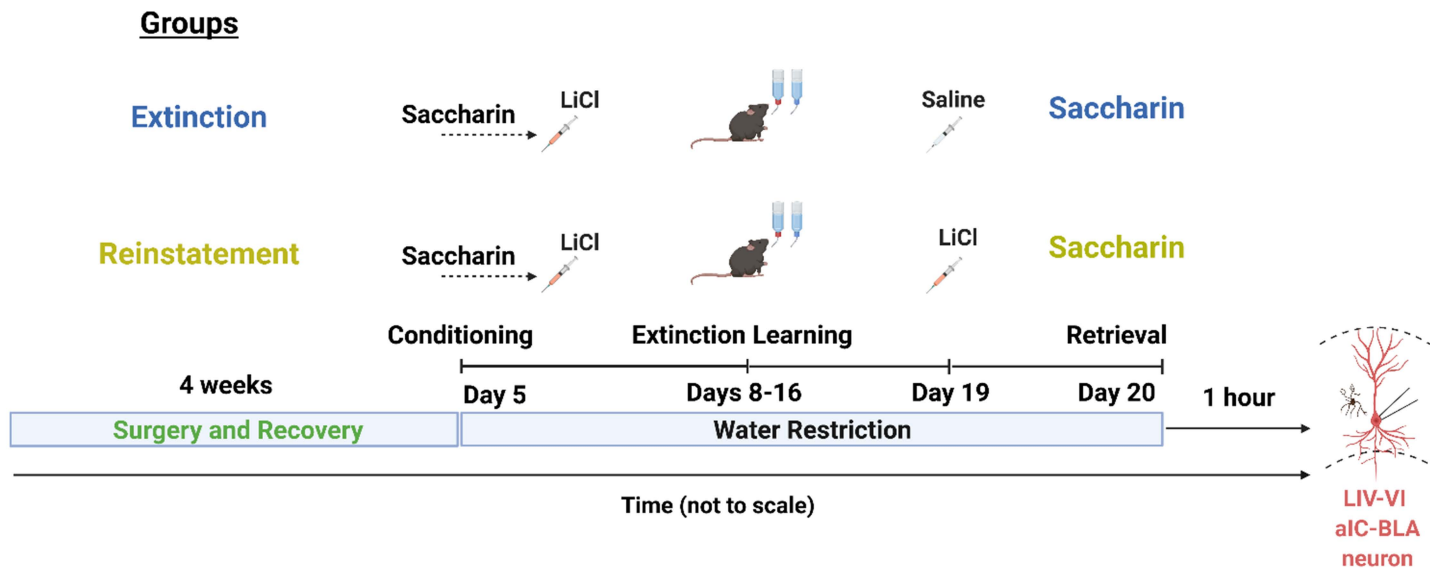


Electrophysiology

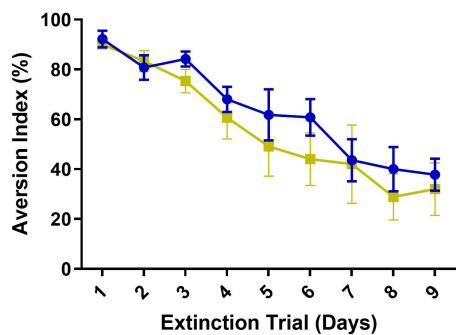


A.

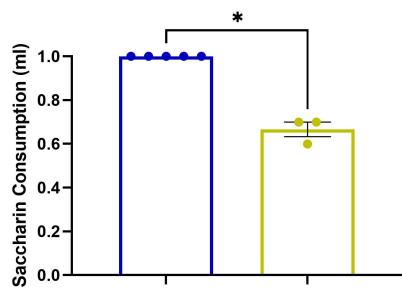
Taste Behavioral Paradigms



B.

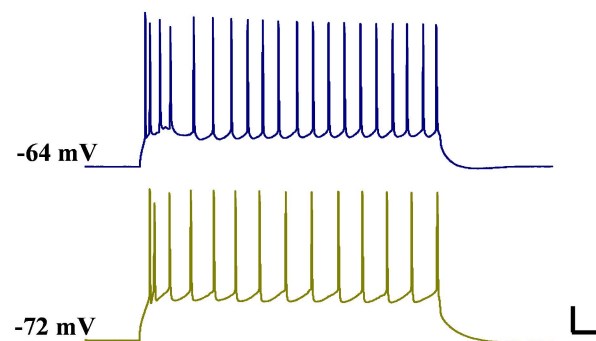


C.

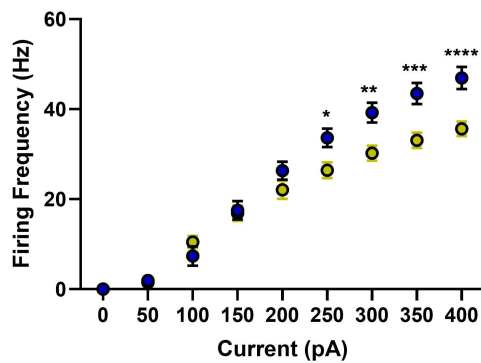


● Extinction ● Reinstatement

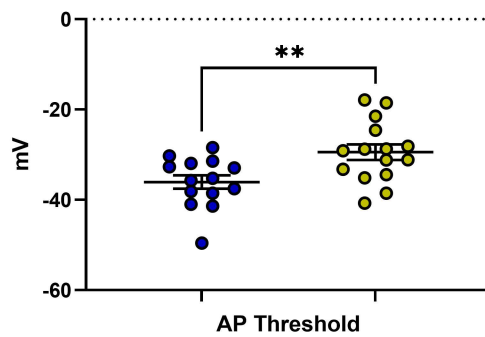
D.



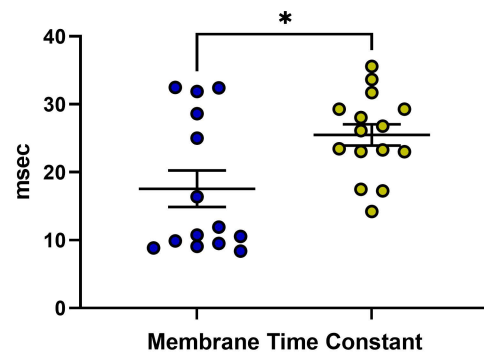
E.

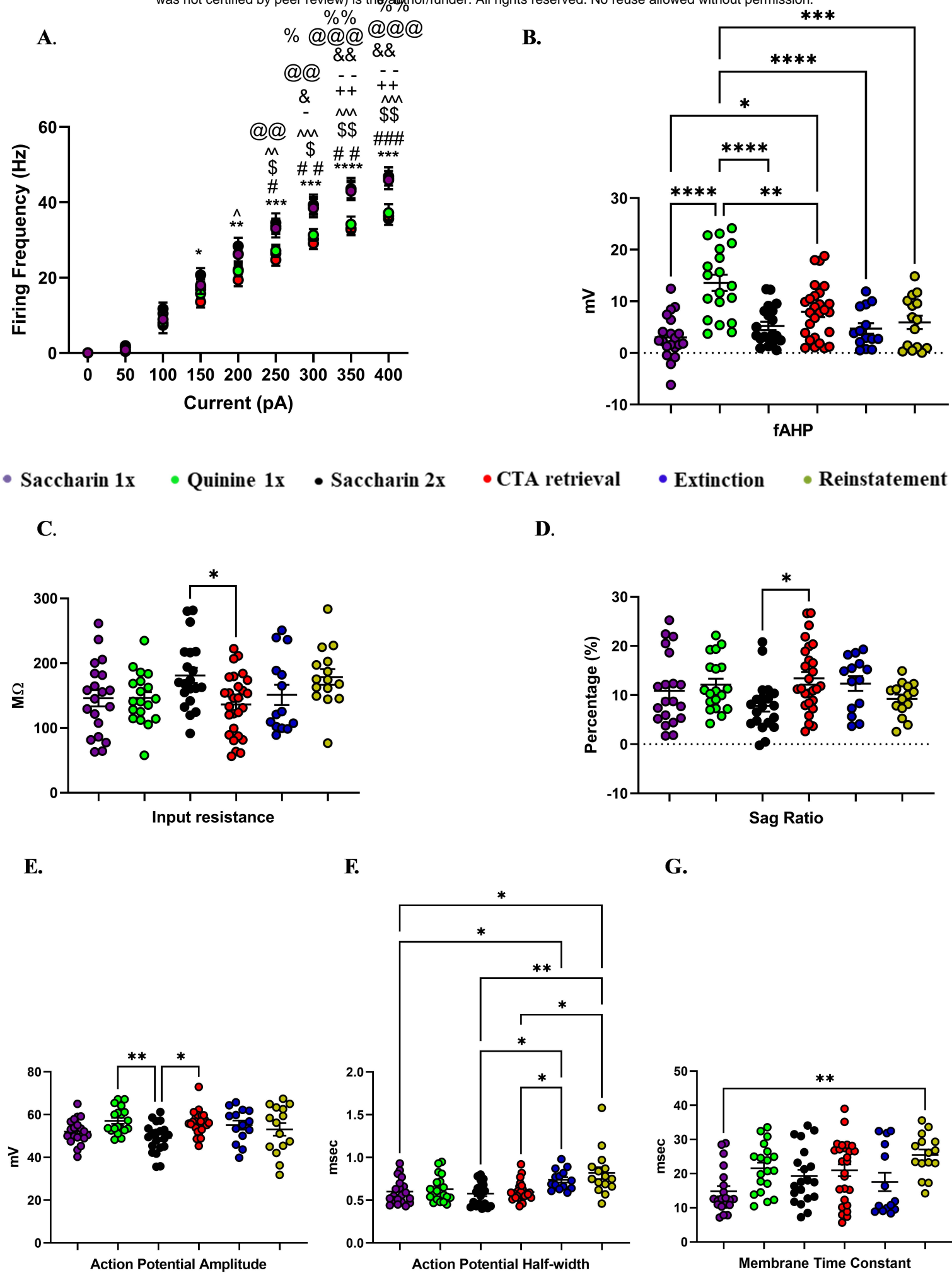


F.



G.

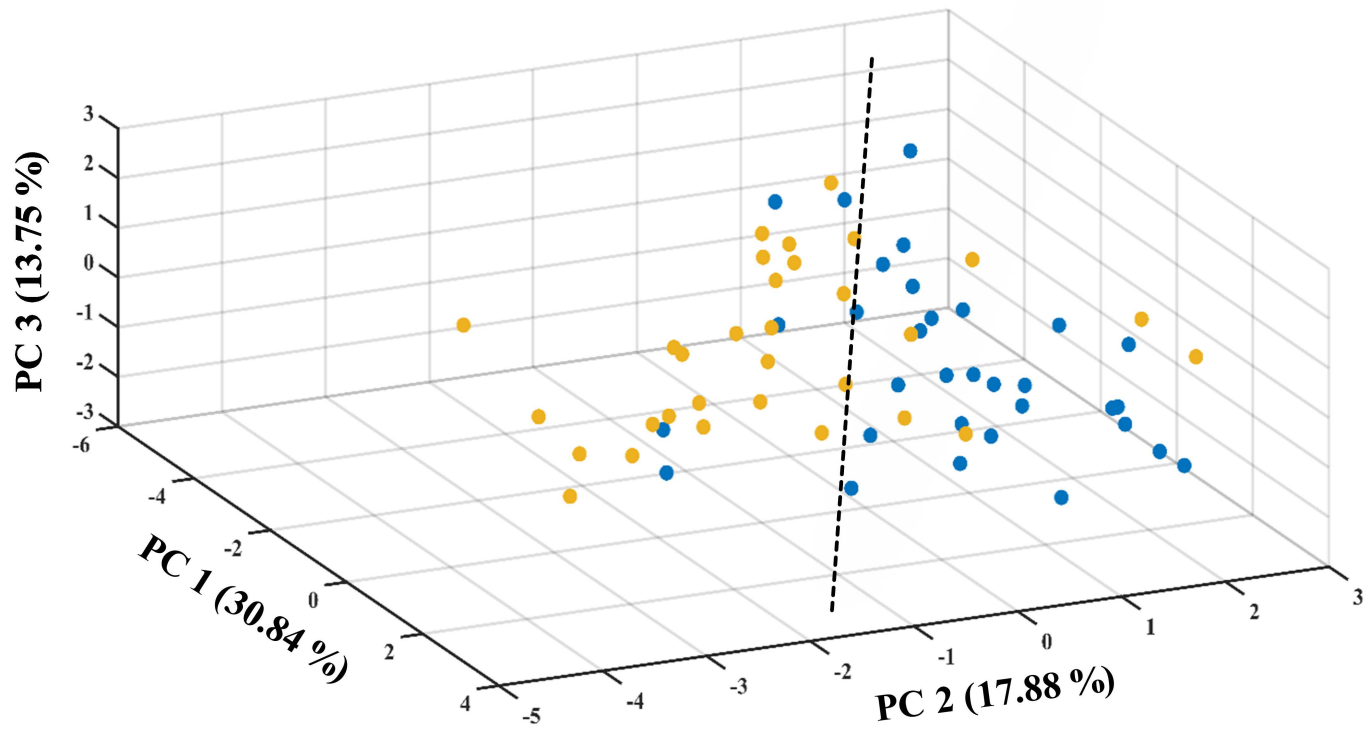




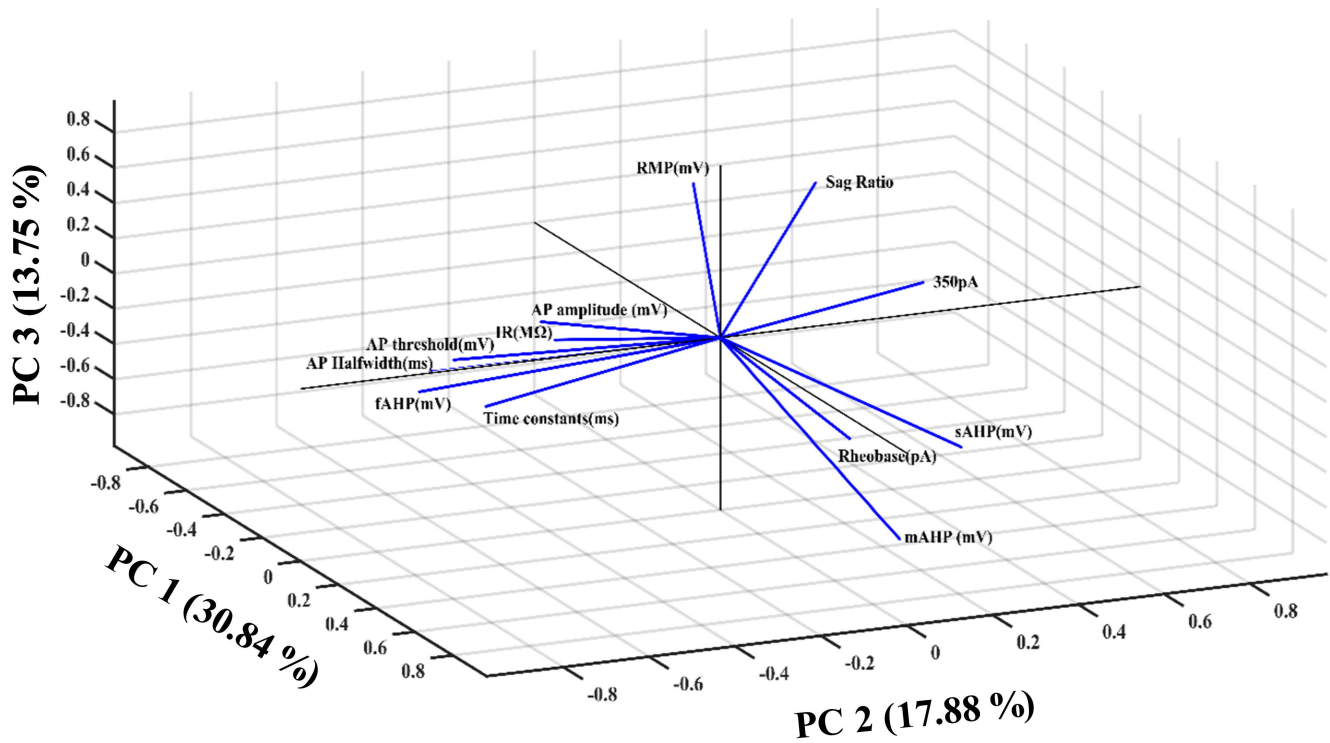
A.

● Low Predictive Following memory

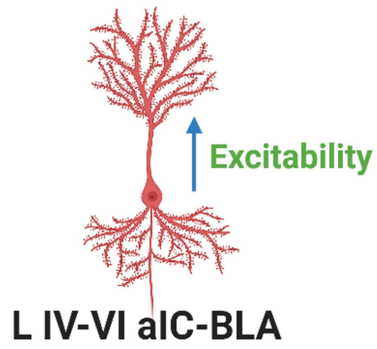
● High Predictive Following memory



B.



Appetitive Novel



Probability of Learning to Avoid



Appetitive Familiar/Aversive

